HINDERED DIFFUSION OF ASPHALTENES AT EVALUATED TEMPERATURE AND PRESSURE

Semi-annual Technical Report

Reporting Period: 03/20/1998 through 09/20/1998

Authors: James A.Guin
Surya Vadlamani

Report Issue Date: 10/03/1998

DE-FG22-95PC95221 -06

Auburn University
Chemical Engineering Department
230 Ross Hall
Auburn University
Auburn, AL 36849

Disclaimer

Abstract

During this time period, the PhD student working on this project, Mr. X. Yang, graduated and has obtained employment with Michelin Tire Company in their research and development laboratory. A new MS student, Mr. Surya Vadlamani, is now working on the project. The work conducted in this time period will form part of Mr. Vadlamani's MS thesis. Also during the current time period, a no-cost extension was obtained for the project, which will allow Mr. Vadlamani to complete the research work required for the MS degree in chemical engineering. Since Mr. Vadlamani was new to the project and in order to provide appropriate training, it was necessary to conduct some experimental work in the same ranges as performed earlier by Mr. Yang in order to provide continuity and insure duplication of the experimental data. The new data obtained by Mr. Vadlamani agree well in general with the earlier data obtained by Mr. Yang and extend the earlier data to a higher temperature range.

Specifically, during this time period, uptake experiments were performed at temperatures from 25^0C to 300^oC for the adsorptive diffusion of quinoline in cyclohexane and mineral oil onto alumina catalyst pellets. These experiments were conducted in a 40 cm^3 microautoclave, as contrasted with the previous work done in the much larger 1-liter autoclave. The use of the microautoclave is more economical from both a purchasing and waste disposal standpoint due to the small quantities of solvents and catalysts utilized, and is also significantly safer at the higher temperatures. Model simulation results showed that the mathematical model incorporating diffusion and adsorption mechanisms satisfactorily fitted the adsorptive diffusion of quinoline onto the alumina catalyst in a fairly wide temperature range of 25^oC to 300^oC. The logarithm of the adsorption constant, obtained by simulating the experimental data with the model solution, was found to be linearly dependent on temperature. The data obtained using the microautoclave agreed well with the previous data obtained using the larger 1-liter autoclave.

HINDERED DIFFUSION OF ASPHALTENES AT ELEVATED TEMPERATURE AND PRESSURE

Table of Contents

Objectives

1. To investigate the hindered diffusion of coal and petroleum asphaltenes in the pores of catalyst particles at elevated temperature and pressure.

2. To examine the effects of concentration, temperature and solvent type on the intraparticle diffusivity of asphaltenes.

Executive Summary

During this time period, the hindered diffusion of quinoline in the pores of catalyst particles at temperatures ranging from 25^0C to 300^0C was studied. For safety and economic reasons, these experimental data were obtained using a microautoclave as constrasted with the previous data which was obtained in a much larger l-liter autoclave . The adsorption constant was determined by fitting the experimental diffusion uptake data with a mathematical model solution. As a result of the simulation, it was found that the logarithm of the adsorption constant was linearly dependent on temperature, and as temperature increased, the amount of adsorption decreased. The simulation results showed that the mathematical model satisfactorily fitted the adsorptive diffusion of quinoline onto alumina over a fairly wide temperature range of 25^0C to 300^0C. The data obtained in the microautoclave system agreed well with the data obtained earlier in the 1-liter autoclave. Using the mathematical parameters obtained by fitting the mathematical model to the experimental data, the model was then utilized to simulate the behavior of the uptake process at a variety of additional conditions for both the quinoline/cyclohexane and quinoline/mineral oil systems.

Introduction

Because many catalytic reactions are carried out at relatively high temperatures and pressures, it is advantageous to seek to understand diffusion and adsorption behavior at elevated temperatures and pressures in order to provide reasonable judgment in catalyst design and process development. However, due to the experimental difficulties involved, very few investigators have studied pore diffusion and surface adsorption at high temperatures and pressures. In one study along this line, Seo and Massoth (1985) investigated effects of temperature on hindered diffusion of polyaromatic model compounds into alumina. These investigators concluded that the hindrance factor K_rK_p was a function of temperature; however, their temperature covered a rather limited range of from 25°C to 50°C.

In the current time period, we investigated effects of temperature on the adsorptive diffusion of quinoline in cyclohexane and mineral oil solvents onto a porous alumina catalyst. The uptake experiments were carried out in a batch microautoclave reactor, with temperature being controlled in a range from 25°C to 300°C.

Experimental Section

1. Materials

In adsorptive diffusion experiments, quinoline (Aldrich) was used as solute and cyclohexane (Aldrich) and light mineral oil (Humco) were used as solvents. A commercial alumina catalyst (Johnson Mathey, Lot #A27E03), with a cylindrical shape, 0.33 cm in diameter and 0.36 cm in length, and having a surface area of 100 m^2/g, was used as the adsorption-diffusion medium. Table 1 gives the properties of the porous alumina.

2. Apparatus and Procedures

The diffusion-controlled adsorptive uptake of mineral oil in cyclohexane and mineral oil onto the alumina was carried out in a microautoclave batch reactor where the alumina particles were supported on a wire mesh which avoided direct contact with the

solution until the experiment was begun by immersing the microautoclave in a heated fluidized sand bath. Prior to immersion, the microautoclave was purged with helium 5 times to remove any air in the system and was pressurized up to 300 psig with helium.

The microautoclave was attached to a horizontal agitator and lowered into a fluidized sand bath at the desired temperature which was controlled by a thermostat and runs were made at fixed time intervals with an initial solute (quinoline) concentration corresponding to 100ng N/ml. The catalyst particles were initially in a dry condition and experiments were conducted for various time intervals, following which the liquid phase was collected and analyzed to determine the concentration of solute remaining in the liquid.

The adsorptive uptakes were conducted at temperatures ranging from 25^{o}C to 300^{o}C. A nitrogen analyzer was used to determine quinoline concentration in the liquid phase in order to determine the amount of solute adsorbed onto the catalyst surface.

HINDERED DIFFUSION MODEL DEVELOPMENT

1. Numerical solution

The diffusional uptake model developed here is based on the previously developed model of Yang (1997) in which solute molecules diffuse into porous particles where they are adsorbed onto the solid surface. For completeness, we have resummarized the essential features of the model in this section of the report. As a result of the diffusion – adsorption (uptake) process, the solute concentration in the liquid bath is depleted. The porous solid particles are modeled as spheres, the equivalent radius of the sphere being based on the ratio of particle volume to external surface area (Ma and Evans, 1968).

Based on the above assumptions, the following mathematical model can be derived (Yang, 1997). The mass balance for the solute in the porous particles is :

$$\frac{\partial\left(K_p e C_s\right)}{\partial t}+\frac{\partial\left(r_p q\right)}{\partial t}=\frac{1}{r^2}\frac{\partial}{\partial r}\left(r^2 D_e \frac{\partial C_s}{\partial r}\right) \qquad (1)$$

with the following initial and boundary conditions:

$$C_{t=0} = C_0 \text{ for all r} \qquad (2)$$

$$\frac{\partial C_s}{\partial r} = 0 \text{ at r = 0} \qquad (3)$$

$$C_{r=R} = C_b(t) \qquad (4)$$

A material balance for the solute in the bath yields :

$$\frac{d\left(V C_b\right)}{dt} = -4\pi R^2 n\left(D_e \frac{\partial C_s}{\partial r}\right)_{r=R} \qquad (5)$$

with an initial condition:

$$C_b = C_i \text{ at t = 0} \qquad (6)$$

In the pore diffusion equation (1), q is the adsorption term. Here a linear adsorption isotherm is assumed as indicated by equation (7).

$$q = KC_s \qquad (7)$$

The following dimensionless variables are defined:

$$x = \frac{r}{R}$$

$$t^* = \frac{D_e}{\left(K_p e + r_p K\right)} \frac{t}{R^2}$$

$$q_s = \frac{C_0 - C_s}{C_0 - C_i}$$

$$q_f = \frac{C_0 - C_b}{C_0 - C_i}$$

With the above dimensionless variables the system of governing equations reduce to :

For the catalyst pellet :

$$\frac{\P q_s}{\P t} = \frac{1}{x^2} \frac{\P}{\P x} \left(x^2 \frac{\P q_s}{\P x} \right) \qquad (8)$$

with the initial and boundary conditions:

$$\text{at } t^* = 0 \qquad q_s = 0 \qquad (9)$$

$$\text{at } x = 1 \qquad q_s = q_f \qquad (10)$$

$$\text{at } x = 0 \qquad q_s = \textit{finite} \qquad (11)$$

For the surrounding solution in the tubing bomb:

$$\frac{dq_f}{dt^*} = -\frac{3}{B} \frac{\P q_s}{\P t^*} \qquad \text{at } x = 1 \qquad (12)$$

with the initial condition:

$$\text{at } t^* = 0 \qquad q_f = 1 \qquad (13)$$

where B is a dimensionless quantity

$$B = \frac{V r_p}{W} \frac{1}{\left(K_p e + r_p K\right)} \qquad (14)$$

The diffusion model can be solved analytically (Bird et al., 1960, p357), and the solution for the dimensionless bath concentration is:

$$q_f = \frac{B}{1+B} + 6B\sum_{k=1}^{k=\infty} \frac{e^{-b_k^2 t^*}}{B^2 b_k^2 + 9(1+B)} \qquad (15)$$

where b_k are the non zero roots of the following equation ;

$$\tan(b) = \frac{3b}{3+Bb^2} \qquad (16)$$

For the linear isotherm the initial concentration inside the catalyst pellet C_0 is given by solving the following equation:

$$K_p V_c C_i e = C_0 K_p V_c e + K C_0 V_c r_p \qquad (17)$$

The above equation is based on the assumption that the pores of the initially dry catalyst pellets are rapidly filled with the initial solution having a solute concentration C_I. Following this initial pore filling process, the solute is assumed to be uniformly distributed between the adsorbed phase and the pore fluid, which are in equilibrium, as expressed by the right side of equation (17). Solving for C_0 from equation (17) yields:

$$C_0 = \frac{C_i}{1 + \frac{K r_p}{K_p e}} \qquad (18)$$

Letting

$$A = \frac{1}{1 + \frac{K r_p}{K_p e}} \qquad (19)$$

yields:

$$q_f = \frac{1}{1-A}\frac{C_b}{C_i} - \frac{A}{1-A} \qquad (20)$$

Substituting for q_f from eqn(23) into eqn(18) gives :

$$\frac{C_b}{C_i} = A + \frac{B(1-A)}{1+B} + 6B(1-A)\sum_{k=1}^{\infty} \frac{e^{-b_k^2 t^*}}{B^2 b_k^2 + 9(1+B)} \qquad (21)$$

where b_k are the roots of equation (16). A root finding algorithm was written in C++ and the above expression was then evaluated given the volume, amount of catalyst and the value of K.

2. *Estimation of Model Parameters*

a. Molecular and effective diffusivities

The molecular diffusivity was estimated from the Stokes-Einstein equation which is given by $D_\infty = \frac{kT}{6\pi\eta r_m}$ (22)

The effective diffusivity, D_e is expressed by

$$D_e = \frac{K_p K_r \varepsilon}{\tau} D_\infty \quad (23)$$

in which K_p and K_r are the hindered diffusion parameters due to steric and hydrodynamic factors respectively. These two hindrance factors are estimated by Ferry's steric equation (24) and Pappenheimer's viscous drag equation (25), respectively, derived for spherical solutes diffusing in cylindrical pores (Yang, 1997).

$$K_p = (1-\lambda)^2 \quad (24)$$

$$K_r = 1 - 2.104\lambda + 2.089\lambda^3 - 0.948\lambda^5 \quad (25)$$

where $\lambda = \frac{d_m}{d_p}$ where d_m is the solute molecule diameter and d_p is the average catalyst pore diameter.

b. Equivalent radius of the sphere

Since the catalyst particles are actually cylindrical, an equivalent spherical radius is defined by:

$$\frac{\frac{4}{3}\pi R_{eq}^3}{4\pi R_{eq}^2} = \frac{R_{eq}}{3} = \frac{\pi R_{cyl}^2 L}{2\pi R_{cyl}^2 + 2\pi R_{cyl} L} \quad (26)$$

The equation for the calculation of equivalent radius is based on the condition that the ratio of the volume of the catalyst pellet to its total available external surface area being expressed as an equivalent sphere is a constant, i. e.

$(V/S)_{sphere} = (V/S)_{cylinder}$

This definition of an equivalent spherical radius for nonspherical particles has been shown to be a valid approximation in this type of analysis (Yang, 1997).

3. *Special cases*

It may appear to the reader that the model developed above has unique behavior in the special cases of A=0 or A =1, e. g. see equation (20). Thus analysis of these special cases is considered below.

Case a. A = 0

When A =0, equation (20) reduces to

$$q_f = \frac{C_b}{C_i} \qquad (27)$$

This case occurs when the catalyst pellets are completely presaturated with the solvent only (no solute), so that the concentration of the solute within the catalyst particle at time t = 0 is $C_0 = 0$.

Case b. A = 1

From equation (19) it can be seen that A=1 implies K=0 and from equation (18) we obtain $C_0 = C_i$. Physically this means that since the initial concentration of the solute in the catalyst particle is equal to the initial concentration of the solute in the surrounding bath, and there is no adsorption (K = 0) , the concentration gradient is zero and there is no diffusion. Thus this particular case is of little physical interest.

4. *Additional theoretical analysis of the model*

In order to better understand the physical behavior as predicted by the mathematical model, some additional analysis of the model was undertaken and is reported in this section of the report.

a. Equilibrium adsorption

The model developed and represented by equation (21) is

$$\frac{C_b}{C_i} = A + \frac{B(1-A)}{1+B} + 6B(1-A)\sum_{k=1}^{\infty} \frac{e^{-b_k^2 t^*}}{B^2 b_k^2 + 9(1+B)}$$

The state of equilibrium for the above system is defined to be the time when there is no change in the concentration gradient and is theoretically reached at infinite time.

At time t=∞ the above equation reduces to

$$\left.\frac{C_b}{C_i}\right|_{t=\infty} = A + \frac{B(1-A)}{1+B} \qquad (28)$$

The percentage amount of solute adsorbed at equilibrium is given by

$$E = \left(1 - \left.\frac{C_b}{C_i}\right|_{t=\infty}\right) x100 \qquad (29)$$

From equations (28) and (29)

$$E = \frac{(1-A)}{(1+B)} x100 \qquad (30)$$

For a given temperature this value of E only depends on A and B which in turn depend only on the value of V/W (the ratio of solution volume to mass of catalyst) since the value of K is constant at a given temperature for a given system.

b. Equilibrium adsorption time

Since the above system reaches equilibrium only at infinite time, it is customary to focus instead on the finite amount of time elapsed when the concentration of the solution decreases to 98% or 95 % of the concentration at infinite time. In other words, the time taken for 98% or 95% of equilibrium adsorption to take place.

The time taken for 98% of equilibrium adsorption can be determined from the following equation:

$$(1 - \left.\frac{C_b}{C_i}\right|_t) = 0.98(1 - \left.\frac{C_b}{C_i}\right|_{t=\infty}) \qquad (31)$$

Substituting equation (28) in equation (21) we obtain

$$\left.\frac{C_b}{C_i}\right|_t = \left.\frac{C_b}{C_i}\right|_{t=\infty} + 6B(1-A)\sum_{k=1}^{\infty} \frac{e^{-b_k^2 t_{98}{}^*}}{B^2 b_k^2 + 9(1+B)} \qquad (32)$$

Substituting equation (32) into equation (31) yields

$$(1 - \left.\frac{C_b}{C_i}\right|_{t=\infty} - 6B(1-A)\sum_{k=1}^{\infty} \frac{e^{-b_k^2 t_{95}{}^*}}{B^2 b_k^2 + 9(1+B)}) = 0.98(1 - \left.\frac{C_b}{C_i}\right|_{t=\infty}) \qquad (33)$$

which reduces to

$$6B(1-A)\sum_{k=1}^{\infty}\frac{e^{-b_k^2 t_{98}^*}}{B^2 b_k^2+9(1+B)} = 0.02\left(1-\left.\frac{C_b}{C_i}\right|_{t=\infty}\right) \qquad (33.a)$$

and similarly for 95% adsorption

$$6B(1-A)\sum_{k=1}^{\infty}\frac{e^{-b_k^2 t_{95}^*}}{B^2 b_k^2+9(1+B)} = 0.05\left(1-\left.\frac{C_b}{C_i}\right|_{t=\infty}\right) \qquad (33.b)$$

The above two conditions were incorporated into the C++ program to evaluate t_{95} and t_{98}. Here again for a given system at a given temperature t_{95} and t_{98} depend only on V/W. Some plots resulting from this analysis will be shown later in this report.

c. Crossover time

It has been found that for a given system the effective and molecular diffusivities increase with temperature but the adsorption constant, K, decreases with temperature. Since these two parameters play a very important role in the adsorption-diffusion process, one might surmise that as temperature changes the combination of these two effects may result in a crossover time at which the concentration ratio of solute in the solution is identical.
The crossover time for two different temperatures T1 and T2 is defined to be the time when

$$\left.\frac{C_b}{C_i}\right|_{T=T1} = \left.\frac{C_b}{C_i}\right|_{T=T2} \qquad \text{at } t = t_c \qquad (34)$$

The following plot illustrates the concept of Crossover time. It shows adsorptive uptake plots for a set of two temperatures (T1, T2). The Crossover point t_c as mentioned above is the time when the adsorptive uptake curves for both the temperatures intersect.

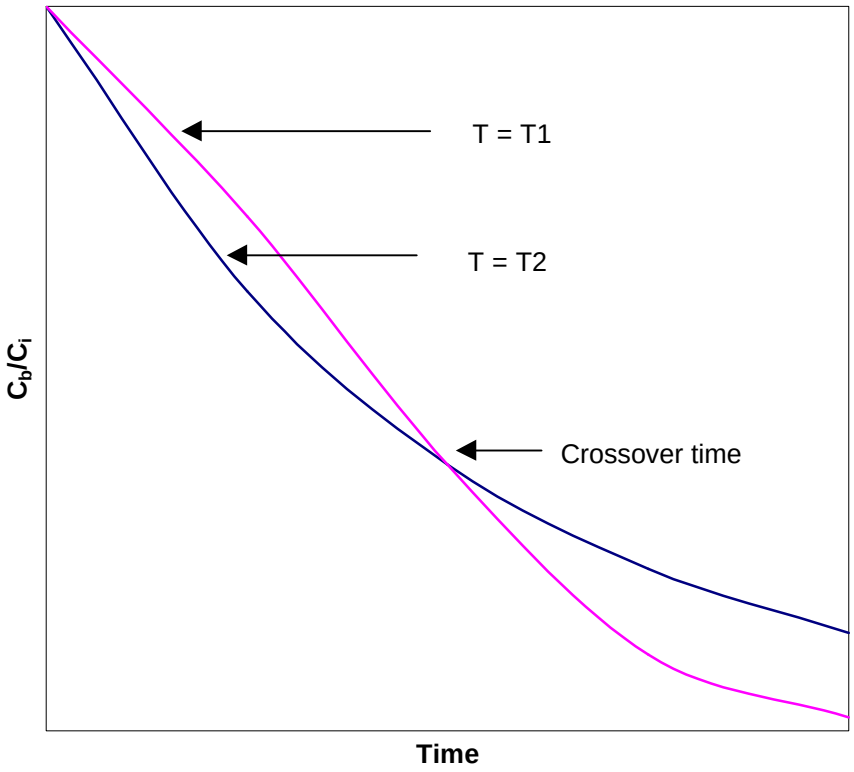

From equations (34) and (21) we obtain

$$A_1 + \frac{B_1(1-A_1)}{1+B_1} + 6B_1(1-A_1)\sum_{k=1}^{\infty} \frac{e^{-b_{1k}^2 t_1^*}}{B_1^2 b_{k1}^2 + 9(1+B_1)}$$

$$= A_2 + \frac{B_2(1-A_2)}{1+B_2} + 6B_2(1-A_2)\sum_{k=1}^{\infty} \frac{e^{-b_{k2}^2 t_2^*}}{B_2^2 b_{k2}^2 + 9(1+B_2)}$$

where

$$t_1^* = \frac{D_{e1}}{\left(K_p e + r_p K_1\right)} \frac{t_c}{R^2}, \quad t_2^* = \frac{D_{e2}}{\left(K_p e + r_p K_2\right)} \frac{t_c}{R^2}$$

$$B_1 = \frac{V_b r_p}{W} \frac{1}{\left(K_p e + r_p K_1\right)}, \quad B_2 = \frac{V_b r_p}{W} \frac{1}{\left(K_p e + r_p K_2\right)}$$

$$A_1 = \frac{1}{1 + \frac{K_1 r_p}{K_p e}} \quad , \qquad A_2 = \frac{1}{1 + \frac{K_2 r_p}{K_p e}}$$

The subscripts denote the parameters at the respective temperatures. The assumption made above is that the solution volume, V and the amount of catalyst, W are the same and the uptake experiments are done with the same catalyst pellets. That is, the only difference in the two simulated experiments is the temperature. Equation (34) was incorporated in the computer program to evaluate the model simulated crossover time, t_c for different values of V/W. The results of this analysis will be discussed in the following section of the report.

Results and Discussion

During the current time period experimental uptake experiments were performed with the systems consisting of quinoline as the adsorptive solute and cyclohexane and mineral oil as the solvents. The experimental data obtained were correlated using the mathematical model as discussed in the previous section.

Quinoline/Cyclohexane system

1. Experimental data

Figure 1 shows a comparison of experimental uptake data taken at 30^o C together with the model predicted curves. The model curves, which are plotted for three different K values, can be used to estimate the appropriate value of K (adsorption constant) at 30^0C as 14.8 cc/g. Actually, this procedure was performed by a least squares method. This value of K was then validated with a different set of experimental conditions (different catalyst loading W) as shown in Figure 2. As shown in Figure 2, the same value of K fits the data well at the second set of experimental conditions. A similar procedure was adopted for experimental data at 50^0C and 100^0C. A comparison of experimental data and validation of the value of K at 50^0C is shown in Figures 3 and 4, respectively. Figures 5 and 6 show the experimental data and validation of the value of K at 100^0C.

For the same V/W ratio the adsorptive uptake decreases with an increase in temperature. It can also be shown from equation (21) that

$$\left.\frac{d}{dt}\left(\frac{C_b}{C_i}\right)\right|_{30^0 C} < \left.\frac{d}{dt}\left(\frac{C_b}{C_i}\right)\right|_{50^0 C} < \left.\frac{d}{dt}\left(\frac{C_b}{C_i}\right)\right|_{100^0 C}$$

at t=0, i.e. the initial adsorption rate increases with increasing temperature.

2. Dependence of viscosity of cyclohexane on temperature

In order to estimate the diffusivity of the solute in the solutions, it is required that the viscosity of the solvent be known. Thus, the viscosity of cyclohexane at three different temperatures is shown in Table 2. By performing a curve fit of this literature data, it is

found that the viscosity decreases with temperature as expected for a liquid, and an exponential relation between h and 1/T is found to fit the data well. The exponential relation obtained is

$$h = 0.059 \exp\left(\frac{1495.8}{T}\right) \tag{35}$$

where h is in cp and T is in Kelvin. This relation yields a linear dependence for the logarithm of viscosity as a function of reciprocal temperature as shown in Figure 7. The linear equation obtained is

$$\ln(h) = \frac{1495.8}{T} - 2.8302 \tag{36}$$

3. *Dependence of molecular and effective diffusivities on temperature*

The molecular diffusivity of quinoline in cyclohexane was estimated from equation (22) which is given by

$$D_\infty = \frac{kT}{6\pi h r_m} \tag{22}$$

For the given system the molecular diffusivity is directly proportional to temperature and inversely proportional to the viscosity of the solvent as shown in the equation above. The effective diffusivity is given by equation (23) which is

$$D_e = \frac{K_p K_r \varepsilon}{\tau} D_\infty \tag{23}$$

The effective diffusivity for the quinoline/cyclohexane system was calculated assuming a tortuosity factor of 3. From equations (22) and (23) it can be seen that the effective diffusivity can be written as

$$D_e = C\frac{T}{h} \tag{37}$$

where C is a constant for the given system and is given by

$$C = \frac{k\varepsilon K_p K_r}{6\pi r_m \tau} \tag{38}$$

For the given quinoline / cyclohexane system the constant C was calculated to be

$C = 3.7 \times 10^{-9}$ g cm^2/s^2 ^{0}K

and thus

$$D_e x 10^6 = 0.0037 \frac{T}{h} \qquad (39)$$

where D_e is in cm^2/s , T is in Kelvin and viscosity in cp. The effective diffusivity from equation (39) is plotted vs. the ratio of temperature/viscosity in Figure 8. Also in Figure 8 is plotted a data point from the previous work by Yang(1997) who used a slightly different method for calculation of the effective diffusivity. Yang's value of D_e is somewhat higher than the value given by equation (39), but is still of the same order of magnitude. The values of molecular and effective diffusivities as computed according to the above equations for the quinoline/cyclohexane system at different temperatures are given also in Table 2.

4. ***Dependence of adsorption constant K on temperature***

The values of K determined by fitting the experimental data at 30, 50, and 100^o C for the quinoline/cyclohexane system are also shown in Table 2. Using these data, a linear relationship was found to exist between ln(K) and temperature and is given by

$$\ln(K) = 11.326 - 0.0288T \qquad (40)$$

The above equation is plotted in Figure 9 with the three data points shown.

5. ***Equilibrium adsorption***

Using the three adsorption constants (K values) at 30, 50, and 100^o C as determined in section 1 above, the percentage equilibrium adsorption E given by equation (30) is plotted as a function of V/W for these three temperatures in Figure 10. The plot covers V/W values in the range from 0 to 100 cc/g although the physically most important values range from around 5-20 cc/g. It can be seen from the plot that for a given temperature as the ratio of V/W increases the percentage equilibrium adsorption decreases. In other words, the amount of solute adsorbed decreases as the amount of catalyst decreases, as expected. It can also be noted that for a given value of V/W the highest percentage equilibrium

adsorption is achieved at the lowest temperature, i. e., as the temperature increases the E factor decreases. This occurs because, as the temperature increases, the adsorption constant K decreases, resulting in a decrease in the equilibrium uptake. On the other hand, an increase in the effective diffusivity D_e at higher temperature tends to increase the uptake rate. These opposing temperature interactions resulting from K and D_e compensate to some extent in the adsorption process.

Figure 11 shows the model simulated adsorptive uptake plot calculated by the computer program for different values of V/W for the quinoline/cyclohexane system at 30^0C. It can be seen from this figure that as the value of V/W decreases, the total amount of solute adsorbed increases, i. e. C_b/C_i decreases. Physically this occurs because if the value of V/W is smaller, there exists more catalyst surface area for a relatively smaller amount of solution and hence a greater amount of the solute can be adsorbed. Figure 12 shows model simulated adsorptive uptake plots for three different values of temperature for the quinoline/cyclohexane system at a fixed value of V/W=10. It can be seen that as the temperature increases the curve flattens more quickly and the total amount of solute adsorbed decreases. It can be seen also that the most adsorption is achieved at T= 30^0C and least at T=100^0C. These changes in adsorptive capacity can be attributed to the value of the adsorption constant K which increases as the temperature decreases as shown earlier in Figure 9.

Quinoline/mineral oil system

1. *Experimental data*

Figure 13 shows a comparison of experimental data with the model predicted curves for the mineral oil system. This plot was used to estimate the value of K at 25^0C as 1975 cc/g. This value of K was then validated with a different set of experimental conditions as shown in Figure 14. Note that the extent of uptake is less in Figure 14 than in Figure 13 due to the larger value of V/W. As in the cyclohexane case, a similar procedure was adopted for experimental data at 150^0C and 300^0C. The comparison of experimental data and validation of the value of K at 150^0C is shown in Figures 15 and 16.

Figures 17 and 18 show the experimental data and validation of the value of K at 100^0C. It can be seen from Figures 14, 16 and 18 that for the same V/W ratio the adsorptive uptake decreases with increase in temperature. This effect is caused by the decrease in the adsorption constant K with temperature. In general, the adsorption constants (K values) for the mineral oil solvent are larger than those for the cyclohexane solvent, at the same temperature. This indicates stronger adsorption of quinoline in the mineral oil solvent.

3. *Dependence of viscosity of mineral oil on temperature*

The viscosity of mineral oil at different temperatures is shown in Table 3. As expected for liquids, it was found that the viscosity decreases with temperature and an exponential relation between h and 1/T was found to fit the data well. The exponential relation obtained was

$$h = 0.003\exp\left(\frac{2612.5}{T}\right) \qquad (41)$$

where h is in cp and T is in Kelvin. A plot of the logarithm of viscosity versus the reciprocal of temperature is shown in Figure 19. The linear dependence of the logarithm of viscosity on the reciprocal of temperature can be expressed by the following equation

$$\ln(h) = \frac{2612.5}{T} - 5.809 \qquad (42)$$

3. *Dependence of molecular and effective diffusivities on temperature*

For the quinoline / mineral oil system the molecular diffusivities are estimated according to the Scheibel relation (Yang, 1997),

$$D_{\infty} = 3.04x10^{-8}\frac{T}{h} \qquad (43)$$

where D_e is in cm^2/s , T is in Kelvin and h is in cp.

The effective diffusivity was expressed as

$$D_e = \frac{K_p K_r e}{t} D_{\infty}$$

It was also found that the dependence of effective diffusivity D_e on temperature could be expressed by the folowing curve fit equation as

$$D_e x10^6 = 20 - 0.1T + 2x10^{-4}T^2 \qquad (44)$$

where D_e is in cm^2/s and T is in Kelvin. A comparison between the present work and Yang's work (1997) on the effective diffusivities for the quinoline/mineral oil system is shown in Figure 20 where good agreement can be observed.

4. *Dependence of adsorption constant K on temperature*

The values of K for different temperatures for the quinoline/mineral oil system are shown in Table 2. A linear relationship was found to exist between ln(K) and temperature as given by

$$\ln(K) = 13.721 - 0.0199T \qquad (45)$$

The above equation is plotted in Figure 21 along with some data points computed from the work by Yang(1997) on the same system. The dependence of K on T agrees with the data from Yang (1997) in a temperature range of 35 - 200^0C. The highest temperature studied by Yang was 200^0C and thus the present work serves to confirm the earlier work by Yang and extends his data for the quinoline/mineral oil system to 300^o C. Using the values obtained by fitting the model to the experimental data, a variety of conditions were investigated using computer model calculations and the results are shown in the following plots. Model simulated plots for the quinoline/mineral oil system with variation of

certain parameters are shown in Figures 22 , 23 and 24. Figure 22 shows the model simulated plot for the % Equilibrium adsorption, E for different values of V/W at 25, 150 and 300^0C. It can be seen that the value of E is highest for the lowest temperature at any given value of V/W. This occurs because at a lower temperature the value of the adsorption constant, K is higher and hence greater adsorption of the solute quinoline takes place. This plot shows that V/W must be less than 100 to achieve significant adsorption at 300^oC.

Figure 23 shows the model simulated time taken for 95% and 98% of equilibrium adsorption to take place for the quinoline/mineral oil system at 25^0C for different values of V/W. It can be seen that as V/W increases the time taken to achieve equilibrium increases rapidly to very large values. It can also be seen that at any given value of V/W the time taken to achieve 98% equilibrium is greater than the time taken to achieve 95% equilibrium. In practice equilibrium adsorptions greater than about 70% are usually not obtained. Figure 24 shows the model simulated crossover times for different values of V/W for the quinoline/mineral oil system for a set of two temperatures (T1=298K, T2=423K). The crossover times for the above system are obtained by solving equation (35) using the C++ program developed to simulate the model. It can be seen that the crossover time t_c increases with V/W.

Conclusions

In this time period the adsorption-diffusion behavior of quinoline, in cyclohexane and mineral oil onto alumina in a microautoclave batch reactor has been studied in the range of 25 - 300^{0}C. This data served to confirm the results of the work by Yang(1997) and extended it to higher temperatures. In agreement with the earlier work by Yang(1997 the adsorptive uptake was found to be dependent on temperature, equilibrium adsorption capacity and the diffusion rate. The logarithm of the adsorption constant was found to be linearly dependent on the temperature. As temperature increased, the value of adsorption constant decreased. On the other hand the effective diffusivity increased with temperature. These off setting dependences resulting from the adsorption constant and the effective diffusivity compensated to some extent in the uptake process. Simulation results showed that the mathematical model satisfactorily fitted the adsorptive diffusion of quinoline onto cyclohexane in a temperature range of 30^{0}C to 100^{0}C and quinoline in mineral oil in a temperature range of 25^{0}C to 300^{0}C.

Table 1. Properties of Alumina

shape	cylindrical
diameter, cm	0.33
length, cm	0.36
equivalent radius, cm	0.17
surface area, m^2/g	100
particle density, g/cm^3	1.47
pore volume, cm^3/g	0.45
porosity, cm^3/cm^3	0.66
average pore diameter, nm	15.6

Table 2. Viscosities of cyclohexane, diffusivities of quinoline, and adsorption constant values for the quinoline/cyclohexane system at different temperatures.

T ^{0}C	$h^{(a)}$ cP	$D_\infty{}^{(b)}$ x 10^6 cm^2/s	$D_e{}^{(c)}$ x 10^6 cm^2/s	K cc/g
30	0.826	7.784	1.351	14.8
50	0.6054	11.34	1.97	6.5
100	0.325	24.425	4.24	1.85

(a) Estimated according to Maxwell's hand book (Maxwell , 1962)

(b) Calculated from equation (22)

(c) Calculated from equation (23) assuming a tortuosity factor of 3.

Table 3. Viscosities of mineral oil, diffusivities of quinoline and adsorption constant values for the quinoline/mineral oil system at several temperatures.

T ^{0}C	$h^{(a)}$ cP	$D_\infty{}^{(b)}$ x 10^6 cm^2/s	$D_e{}^{(c)}$ x 10^6 cm^2/s	K cc/g
25	19.25	0.4706	0.08169	1975
150	1.4	9.185	1.594	295
300	0.2865	60.8	10.554	8.25

(a) Estimated according to Maxwell's hand book (Maxwell, 1962)

(b) Calculated from Scheibel relation (Perry and Green, 1984) (equation (44))

(c) Calculated from equation (23) assuming a tortuosity factor of 3.

Nomenclature

Letters

A	dimensionless diffusion model parameter
B	dimensionless diffusion model parameter
C_0	solute bath concentration at the center of the particle, g/cm^3
C_b	solute bath concentration, g/cm^3
C_i	initial solute bath concentration, g/cm^3
C_s	solute bath concentration at the surface of the particle, g/cm^3
d_m	solute diameter, cm
d_p	average catalyst pore diameter, cm
$D\infty$	solute molecular diffusivity, cm^2/s
D_e	solute effective diffusivity, cm^2/s
k	Boltzmann constant, 1.38×10^{-16} erg/K
K	linear adsorption constant , cc/g
K_p	partition factor
K_r	restriction factor
r	radial position of the catalyst particle, cm
r_m	solute radius, cm
R	catalyst particle radius, cm
R_{eq}	equivalent radius of the sphere, cm
t	diffusion time, s
t^*	dimensionless time
T	absolute temperature, K
V	catalyst pellet volume, cc
V_b	bath volume, cc
V_p	catalyst pore volume, cc
W	catalyst weight

Greek

e	catalyst porosity
h	solvent viscosity, g/cm-s
q_s	dimensionless concentration in the pores
q_f	dimensionless bath concentration
l	ratio of solute molecule diameter to catalyst pore diameter
x	dimensionless radial position
r	solvent density, g/cm^3
r_p	catalyst particle density, g/cm^3
t	dimensionless time

References

1. Bird, R. B., W. E. Stewart, and E. N. Lightfoot, " Transport Phenomena ", John Wiley & Sons, Inc. 1960.

2. Carl L. Yaws, Handbook of Viscosity, Gulf Publishing Company, Vol 3, p227, 1995.

3. DOE Report No. 95221r02, 1996: "Hindered Diffusion of Asphaltenes at Elevated Temperature and Pressure".

4. DOE Report No. 95221r04, 1997: "Hindered Diffusion of Asphaltenes at Elevated Temperature and Pressure".

5. DOE Report No. 95221r03, 1997: "Hindered Diffusion of Asphaltenes at Elevated Temperature and Pressure".

6. DOE Report No. 95221r05, 1998: "Hindered Diffusion of Asphaltenes at Elevated Temperature and Pressure".

7. Ma, Y. H., and L. B. Evans, AIChE J., 14, 956 (1968).

8. Maxwell J.B. , " Data Book on Hydrocarbons", Standard Oil Development Company, Vol 7, p164, 1962.

9. Seo, E., and F. E. Massoth, AIChE Journal, 31, 494 (1985).

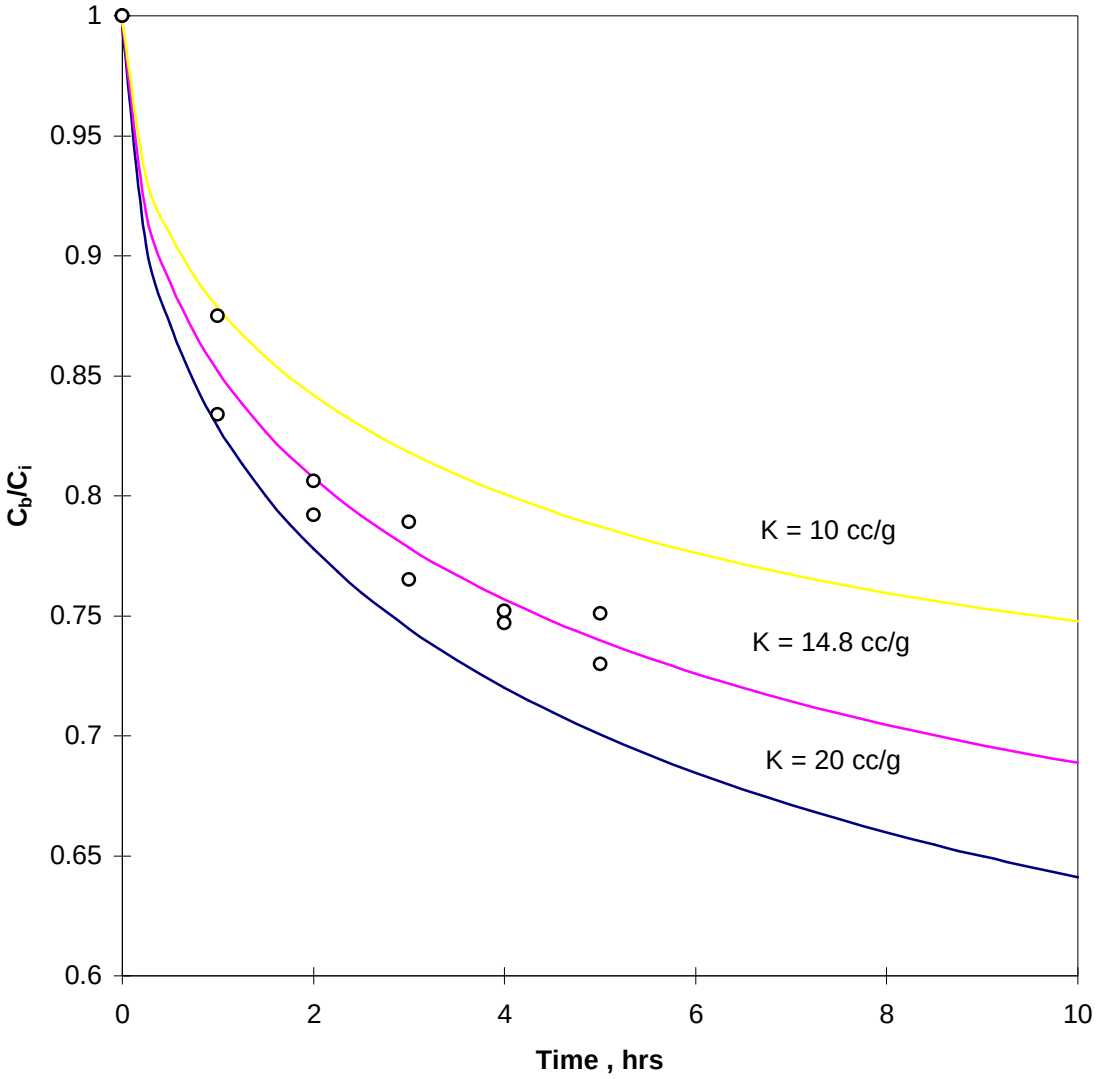

Figure 1. Comparison of experimental data and model simulation for the adsorptive uptake of quinoline in cyclohexane onto alumina (V=4.97ml, W=0.205g, T=30^{o}C).

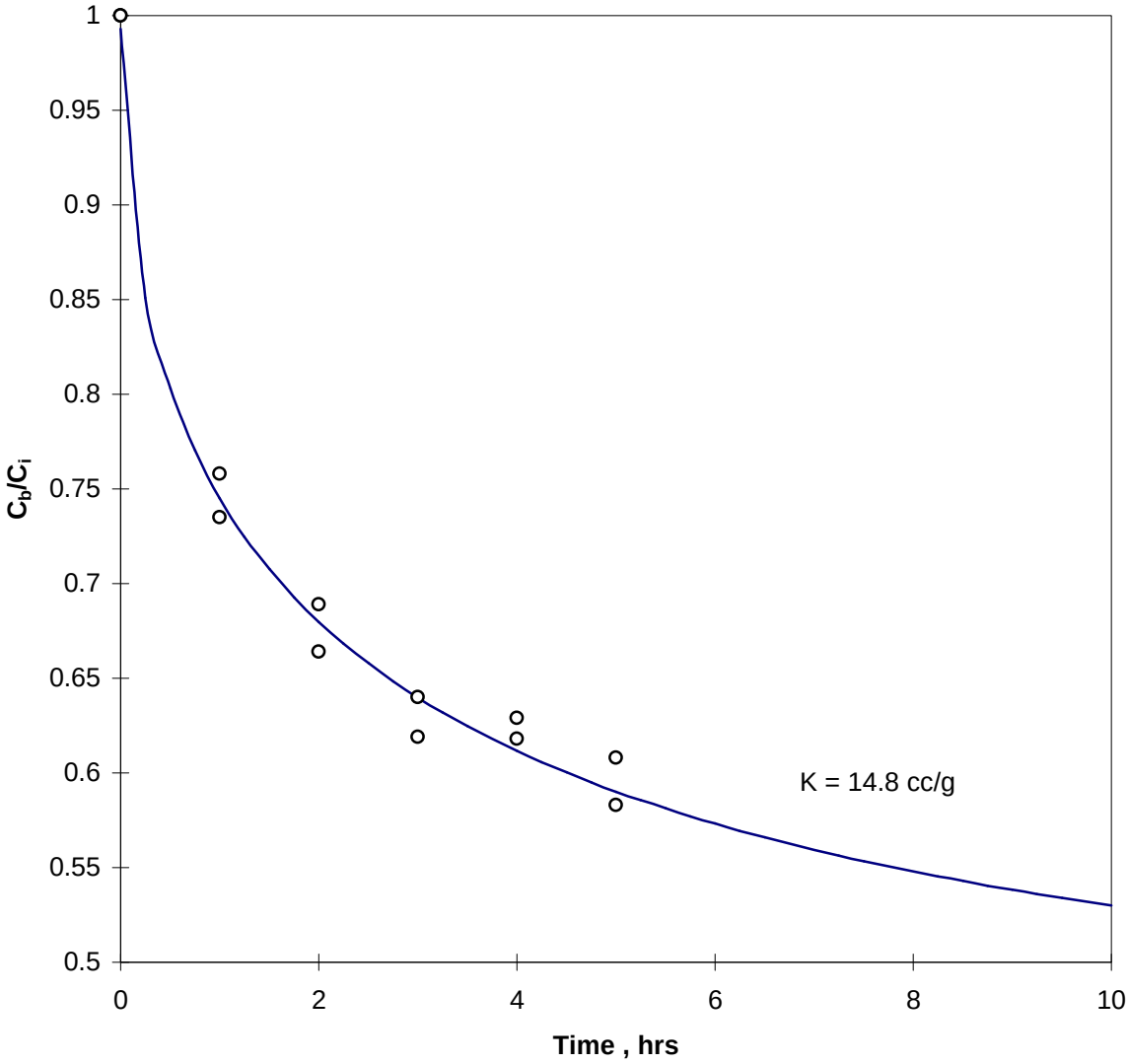

Figure 2. Validation of the value of K for the quinoline/cyclohexane system (V=4.97ml,W=0.395g, T=30^{o}C).

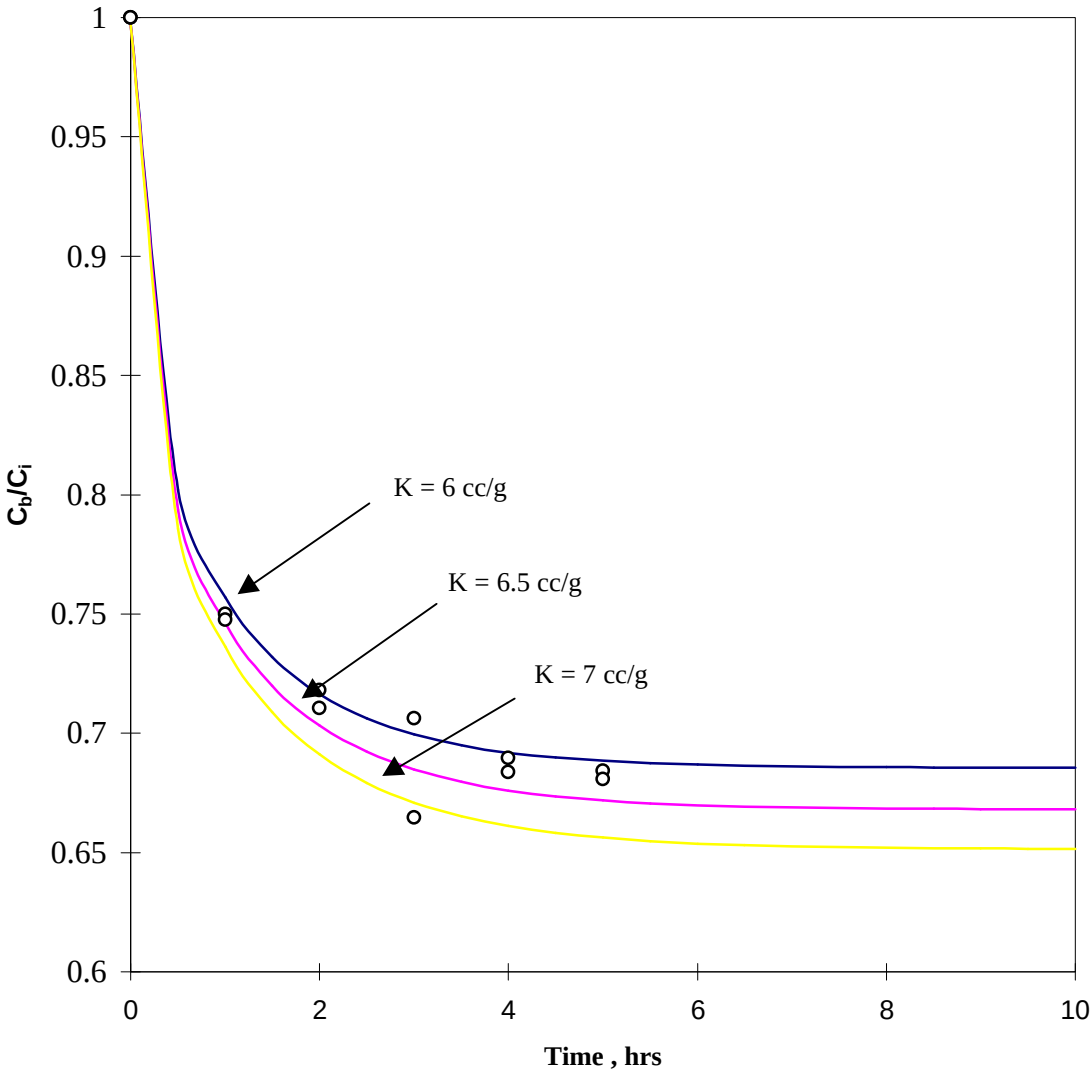

Figure 3. Comparison of experimental data and model simulation for the adsorptive uptake of quinoline in cyclohexane onto alumina (V=4.97ml, W=0.395g, T=50^{o}C)

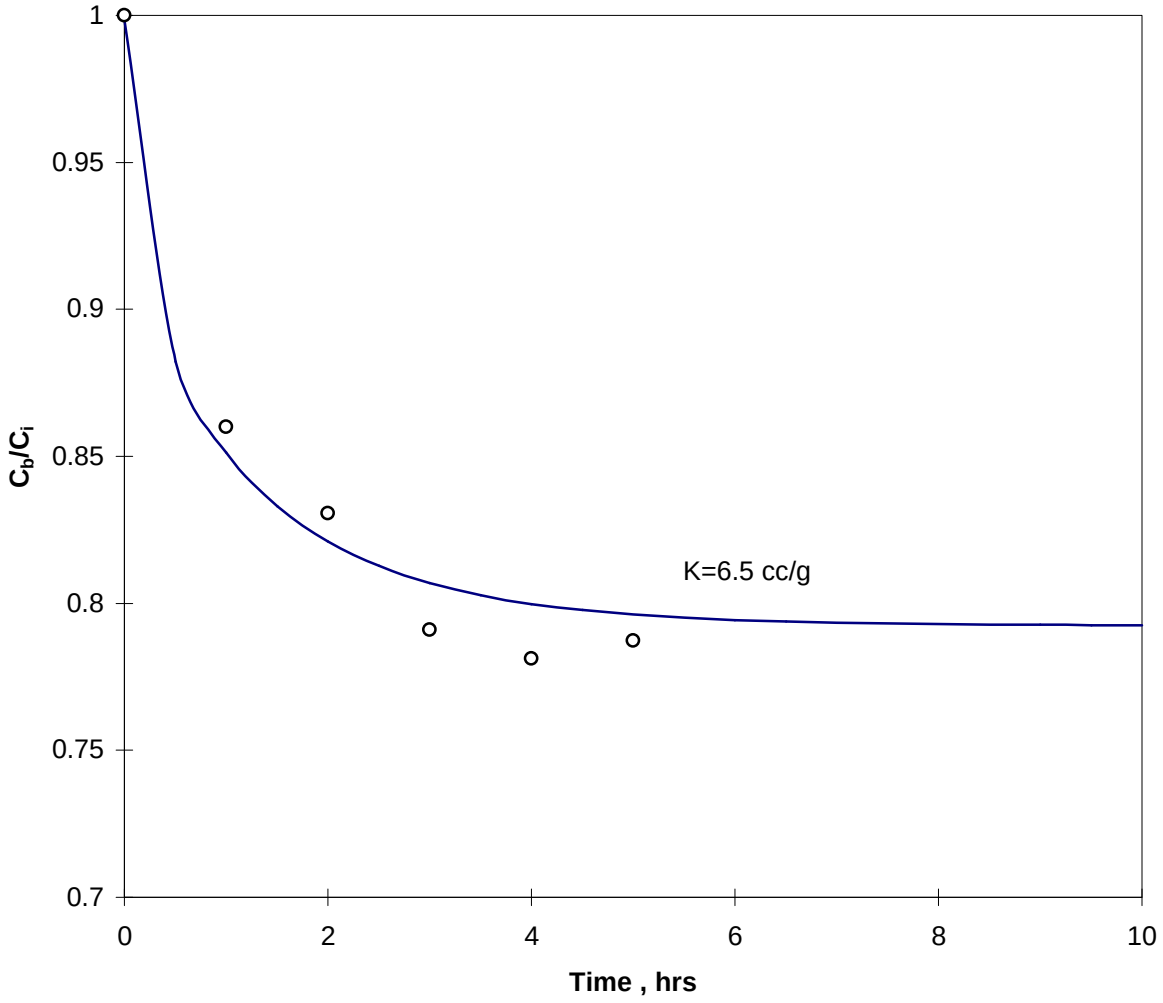

Figure 4. Validation of the value of K for the quinoline/cyclohexane system (V=4.97ml,W=0.205g, T=50^{o}C).

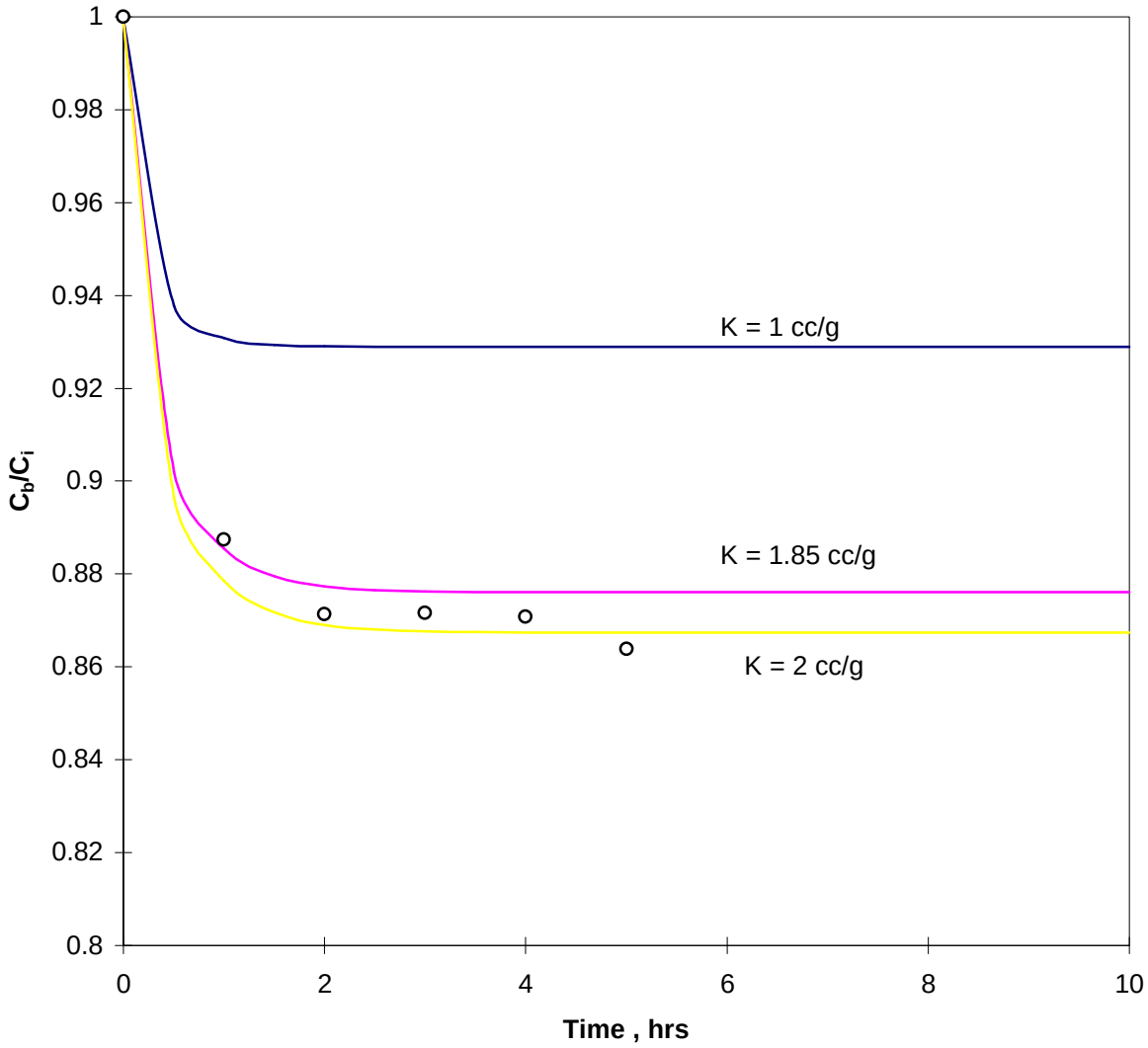

Figure 5. Comparison of experimental and model simulation for the adsorptive uptake of quinoline in cyclohexane onto alumina (V=4.97ml, W=0.395g, T=100^{o}C).

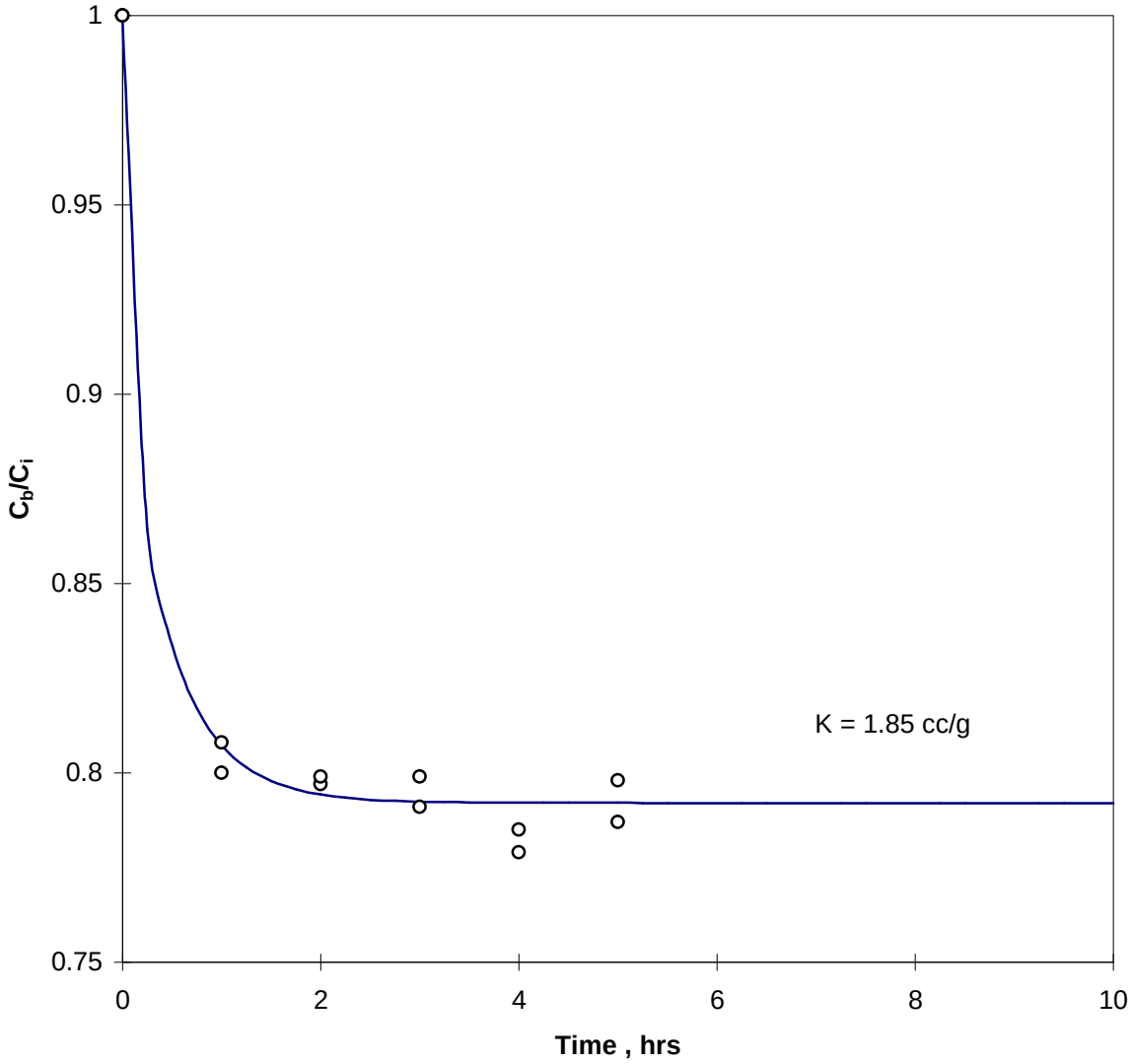

Figure 6. Validation of the value of K for the quinoline/cyclohexane system (V=4.97ml,W=0.75g, T=100^{o}C).

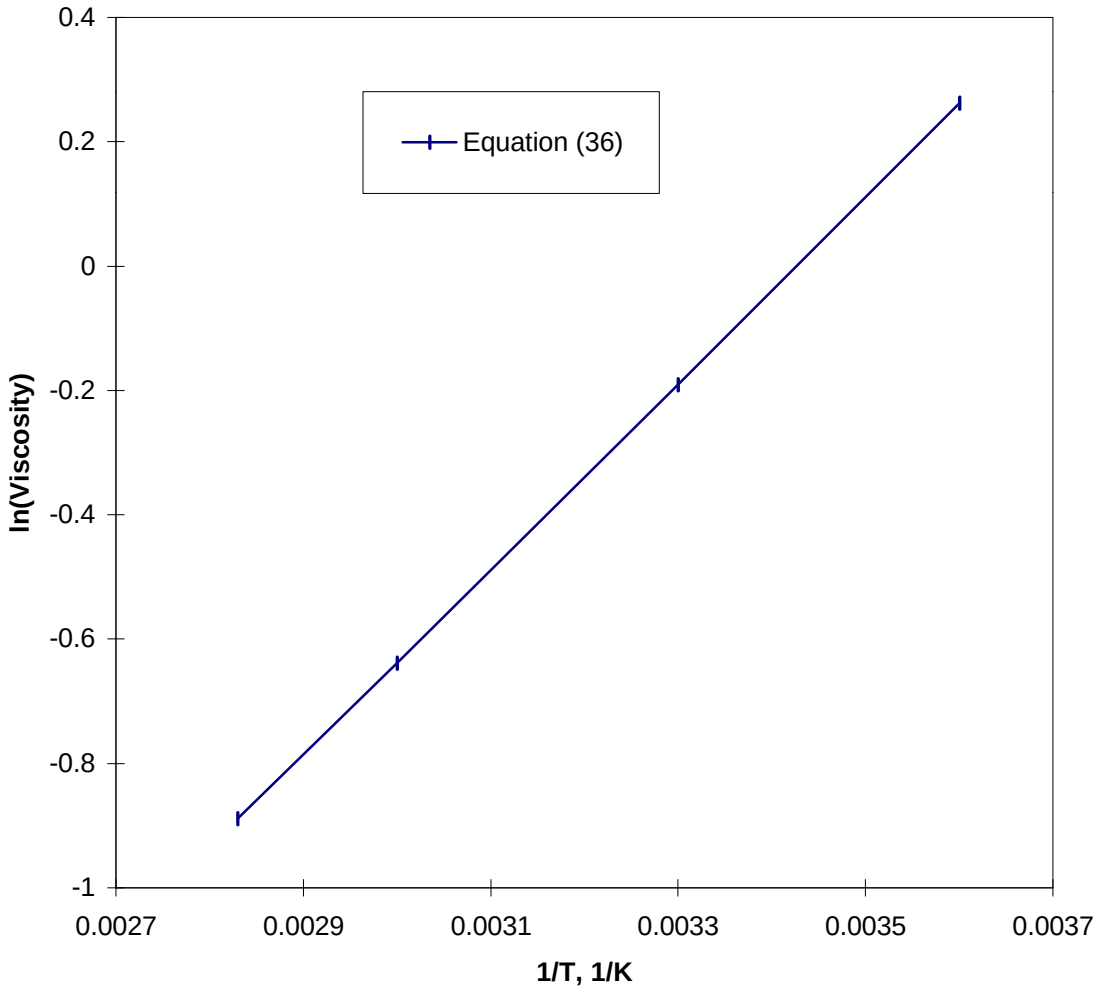

Figure 7. Temperature dependence of the viscosity of cyclohexane.

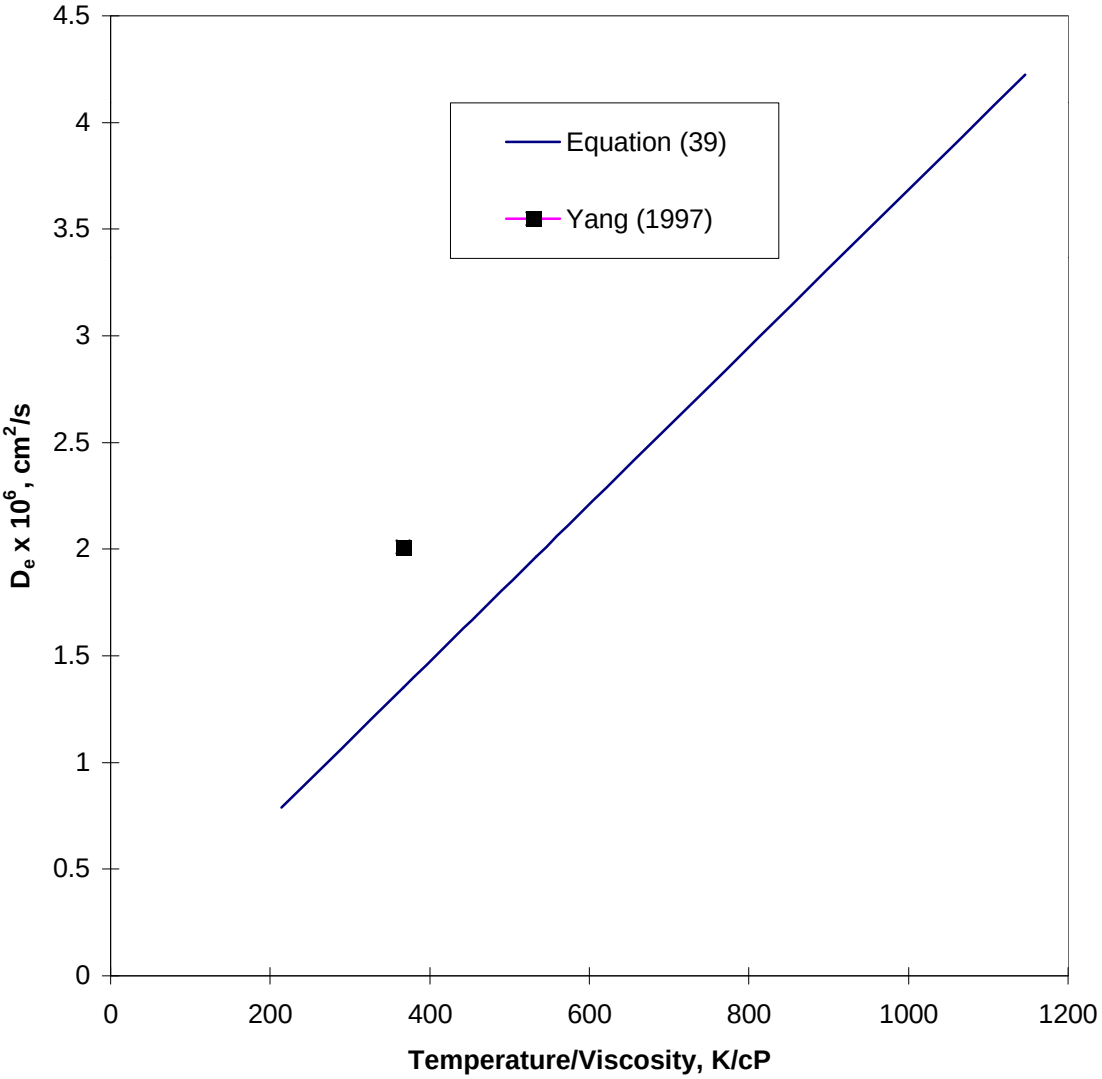

Figure 8. Effective diffusivity of quinoline in cyclohexane as a function of the ratio of temperature to viscosity of cyclohexane.

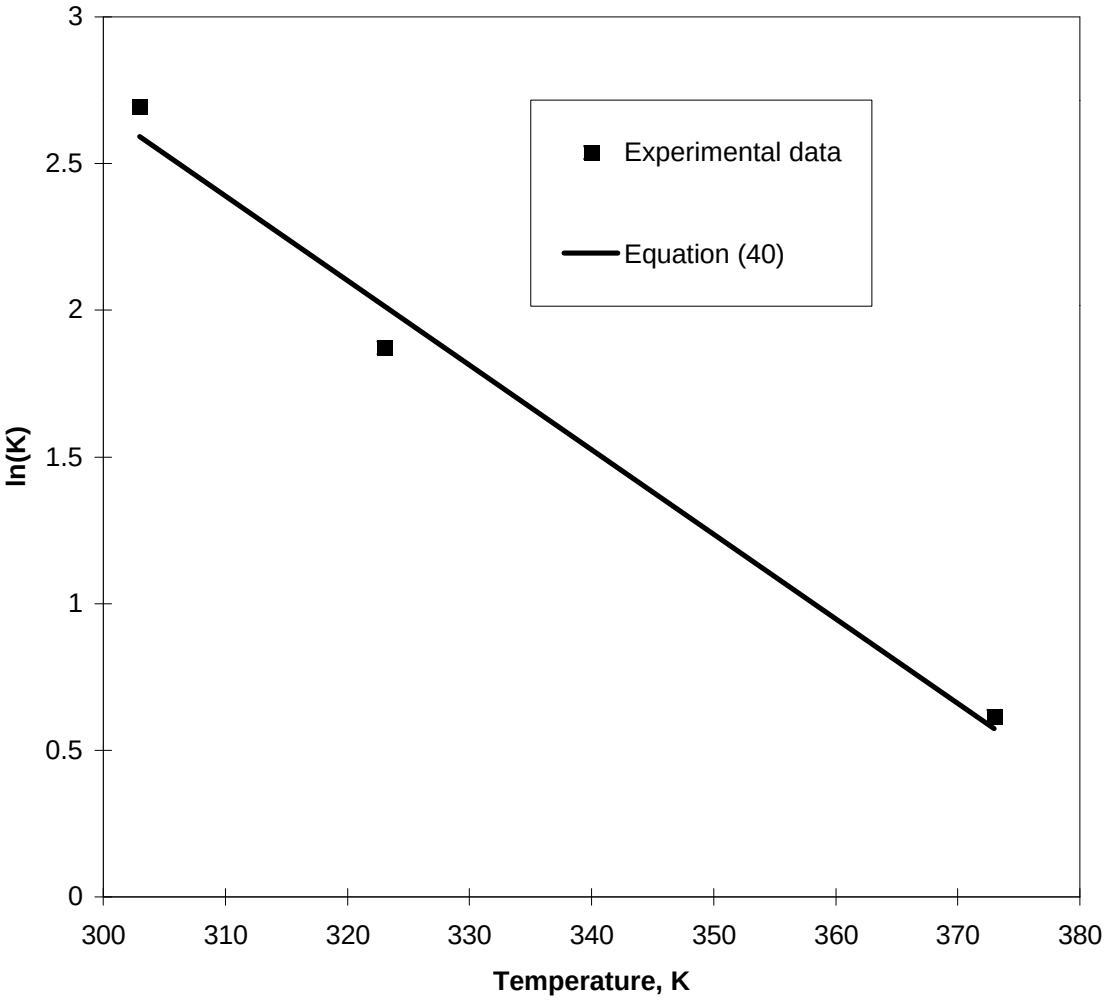

Figure 9. Dependence of the adsorption constant K on temperature for the quinoline/cyclohexane system.

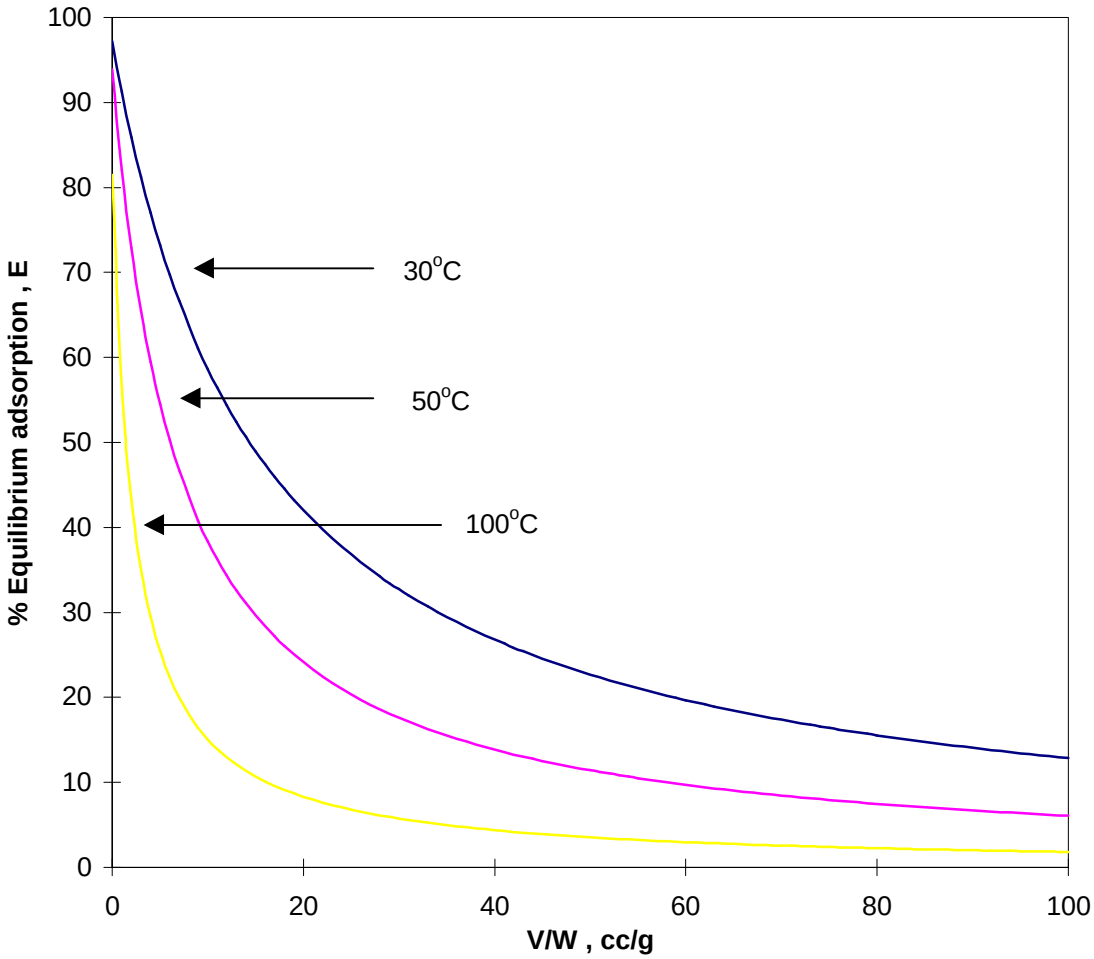

Figure 10. Percentage equilibrium adsorption as a function of V/W for different temperatures for the quinoline/cyclohexane system.

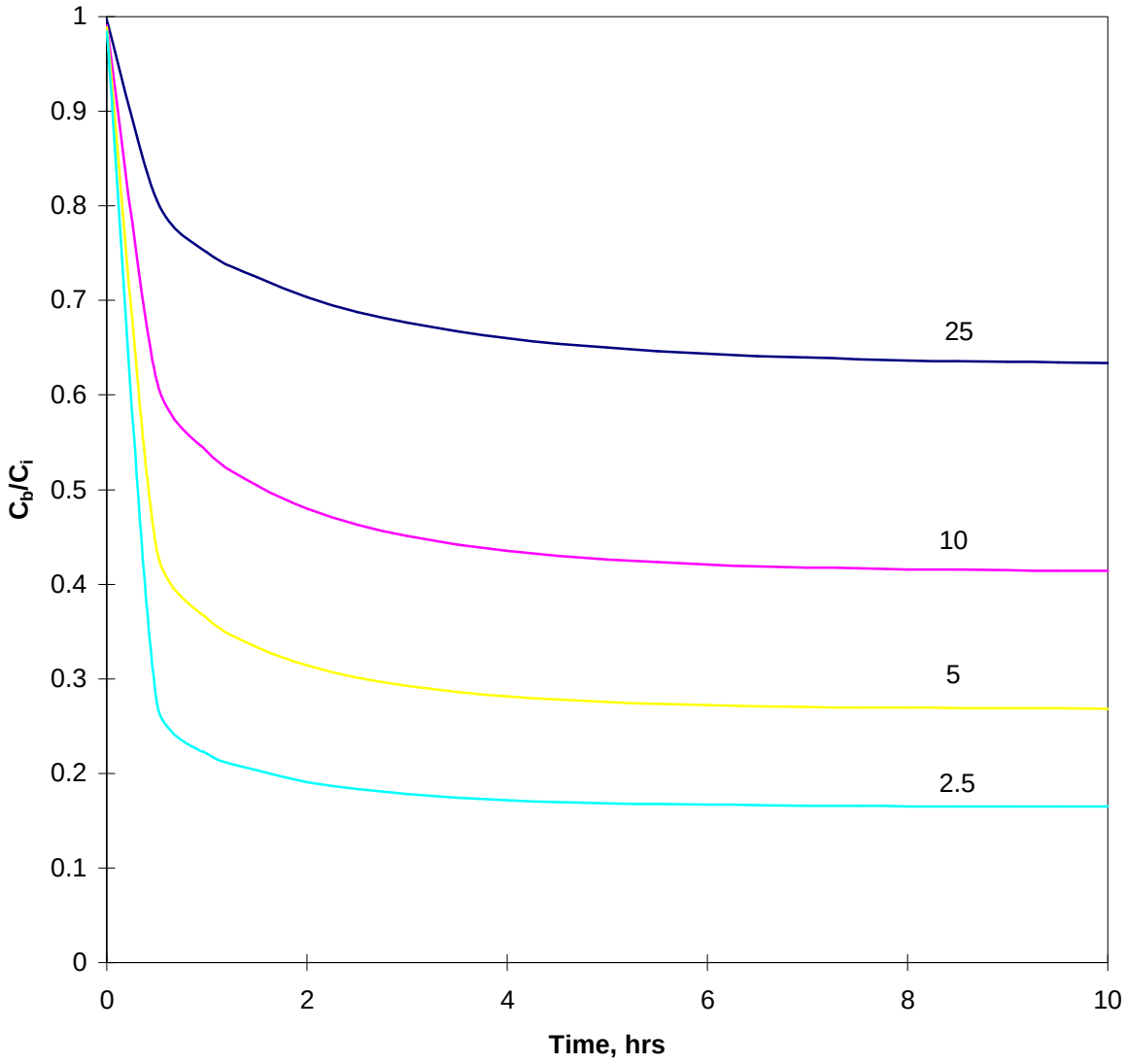

Figure 11. Model simulated uptake plots for different values of V/W for the quinoline/cyclohexane system at 30^{o}C (K=14.8cc/g).

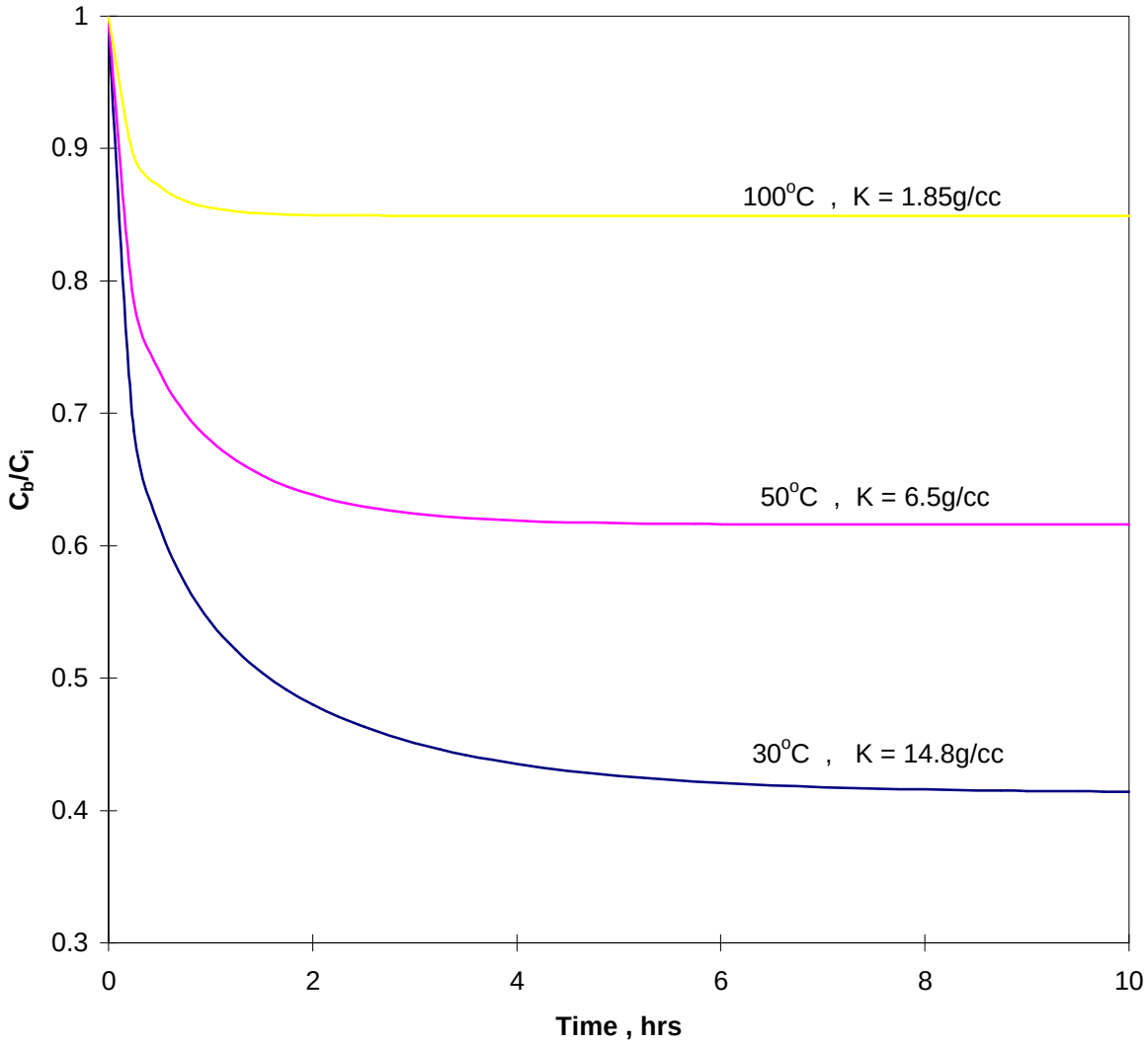

Figure 12. Model simulated uptake plots at different temperatures and a V/W value of 10 for the quinoline/cyclohexane system.

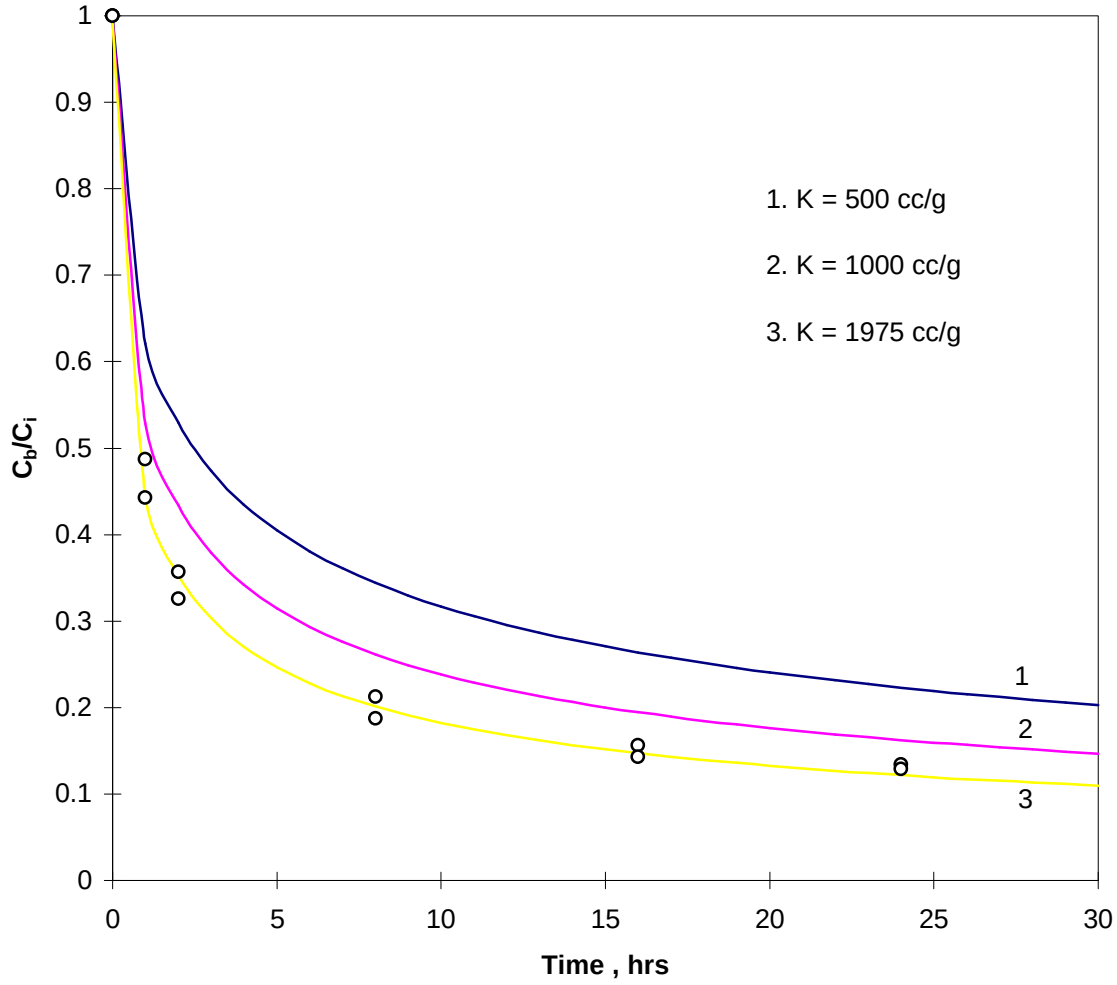

Figure 13. Comparison of experimental data and model simulation for the adsorptive uptake of quinoline in mineral oil onto alumina (V=4.8ml, W=0.395g, T=25^{o}C).

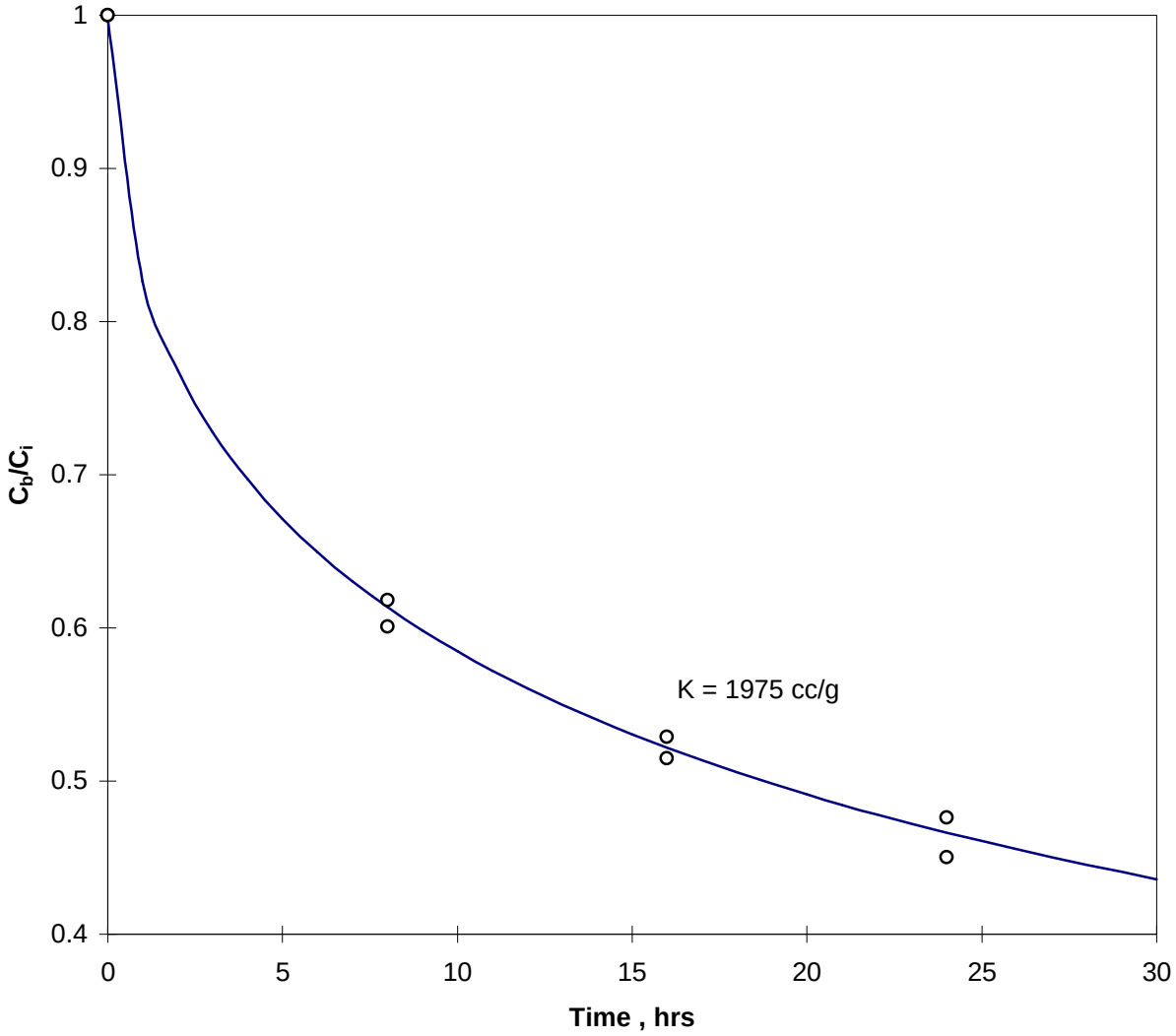

Figure 14. Validation of the value of K for the quinoline/mineral oil system (V=6.95ml, W=0.1g, T=25^{o}C).

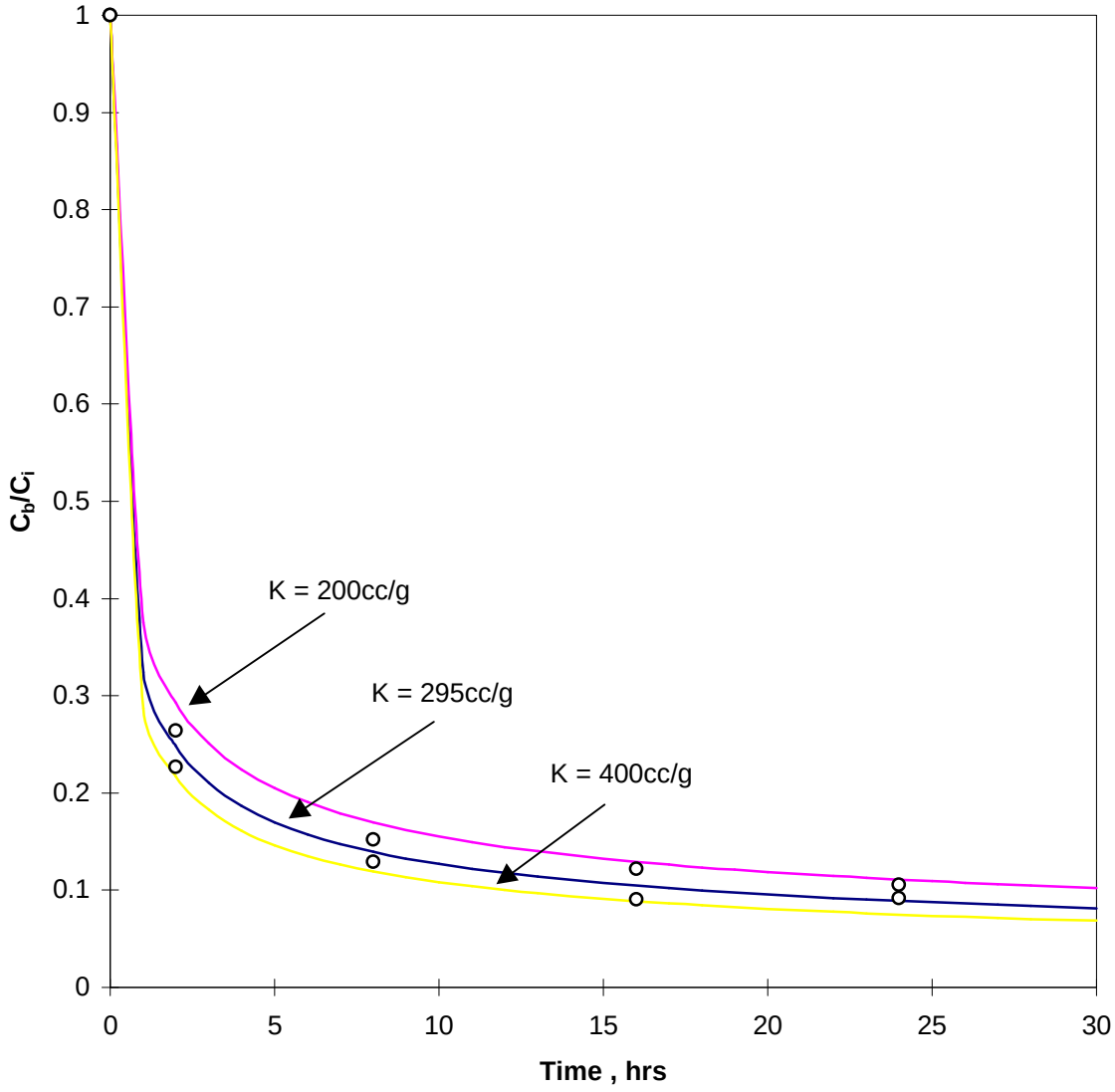

Figure 15. Comparison of experimental data and model simulation for the adsorptive uptake of quinoline in mineral oil onto alumina (V=4.8ml, W=0.395g, T=150^{o}C).

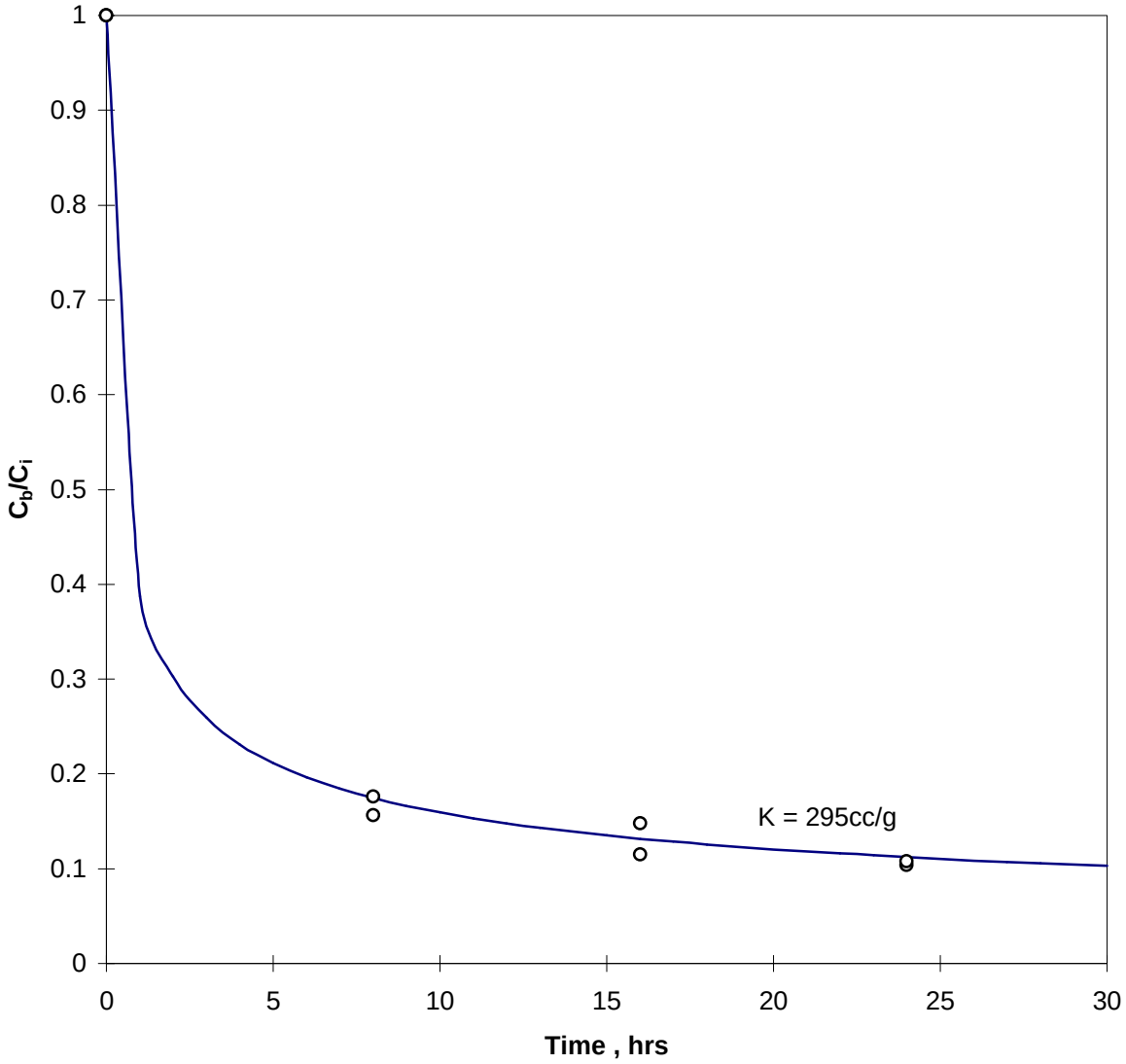

Figure 16. Validation of the value of K for the quinoline/mineral oil system (V=7.7ml, W=0.495g, T=150^{o}C).

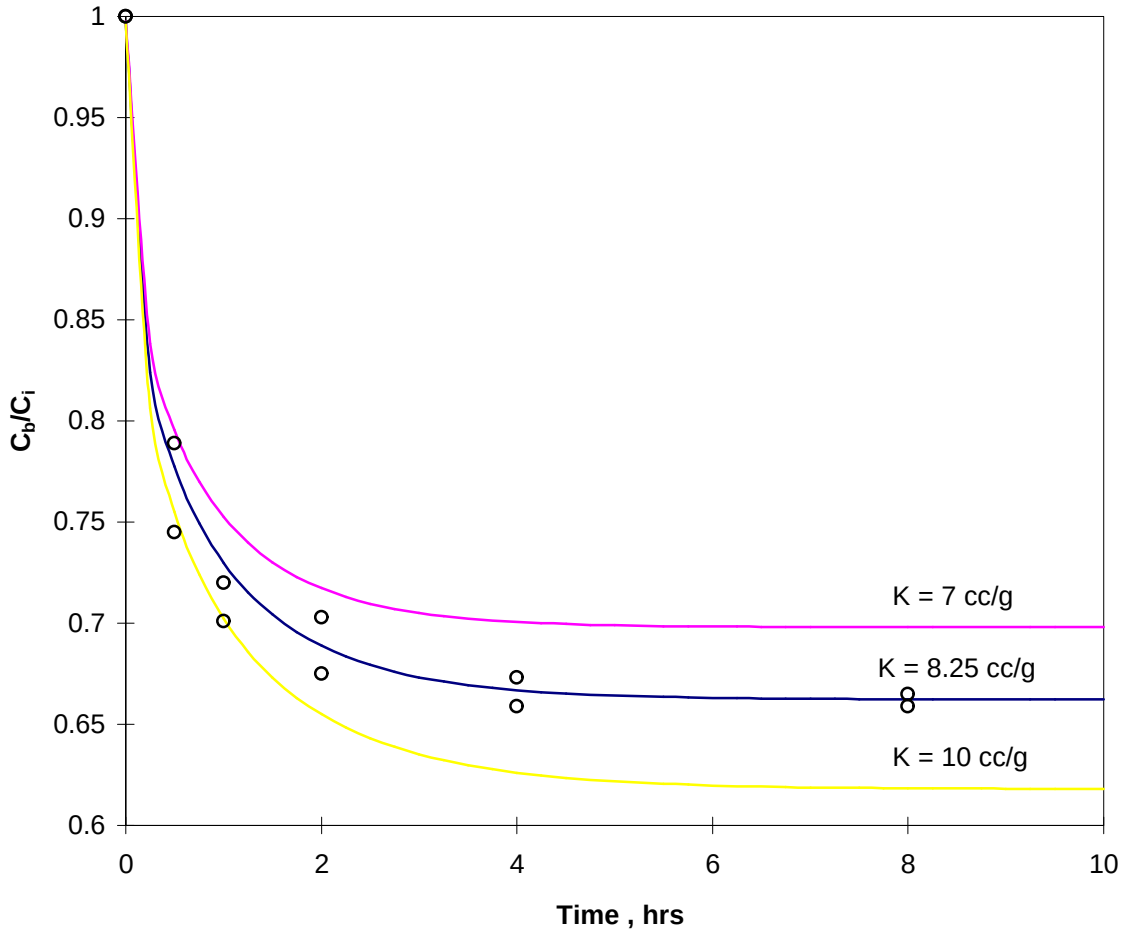

Figure 17. Comparison of experimental data and model simulation for the adsorptive uptake of quinoline in mineral oil onto alumina (V=7.8ml, W=0.495g, T=300^{o}C).

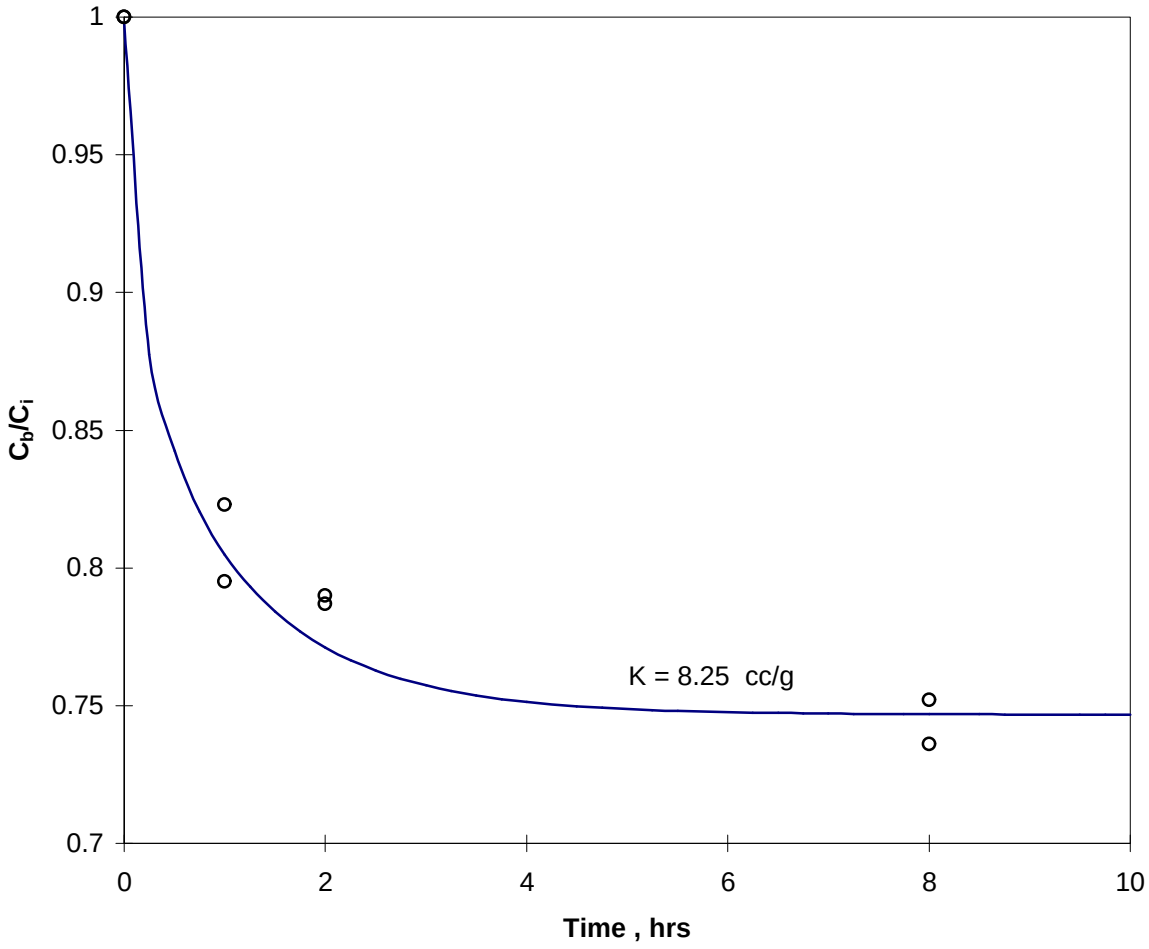

Figure 18. Validation of the value of K for the quinoline/mineral oil system (V=4.9ml, W=0.205g, T=300^{o}C).

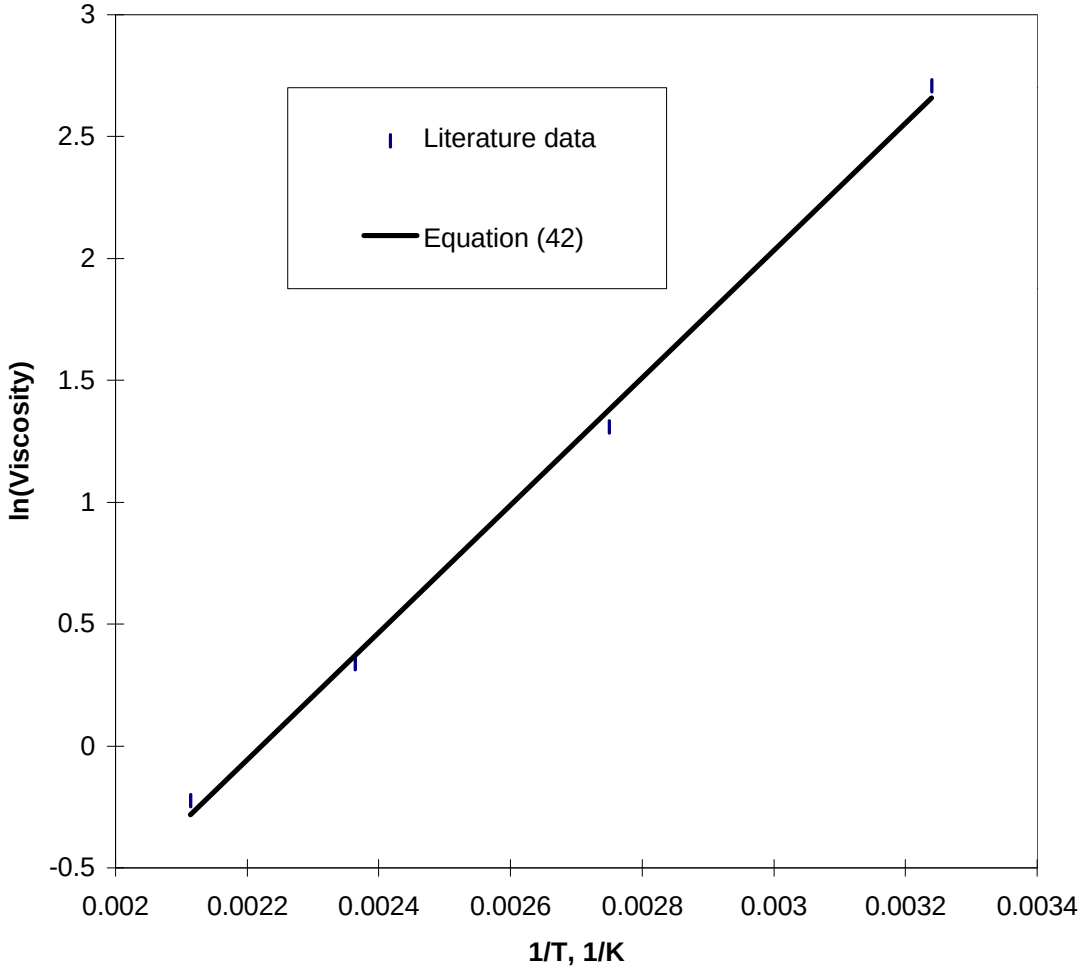

Figure 19. Temperature dependence of the viscosity of mineral oil.

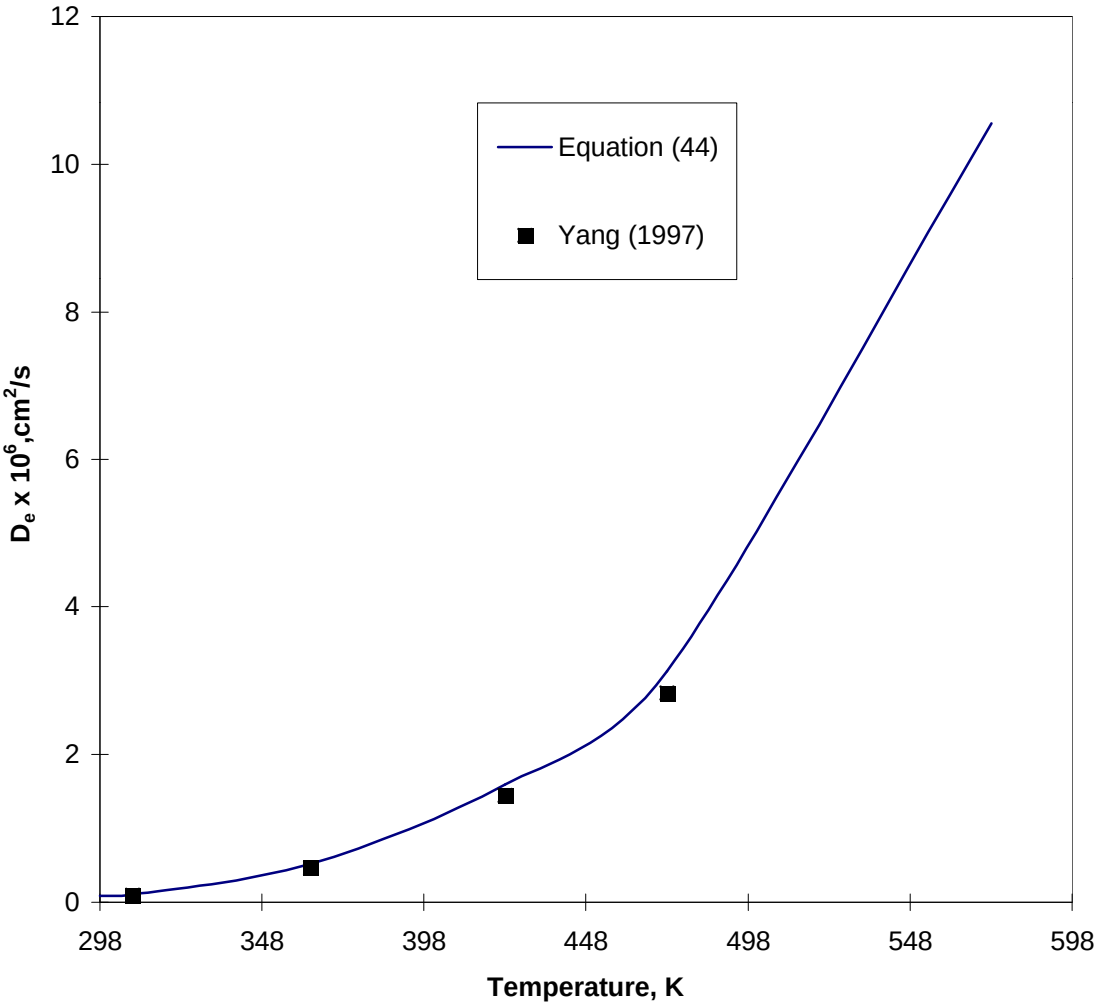

Figure 20. Effective diffusivity of quinoline in mineral oil versus temperature.

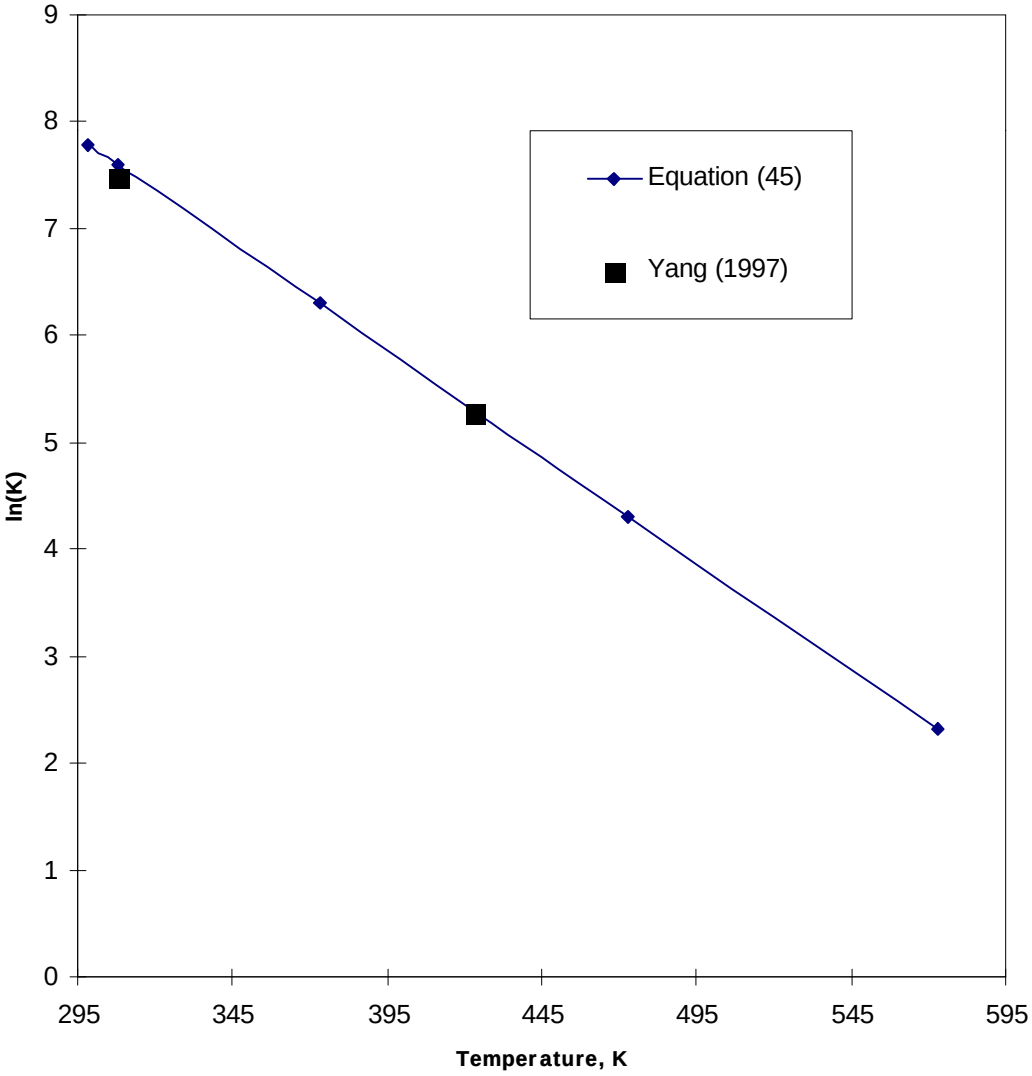

Figure 21. Temperature dependence of the adsorption constant for the quinoline/mineral oil system.

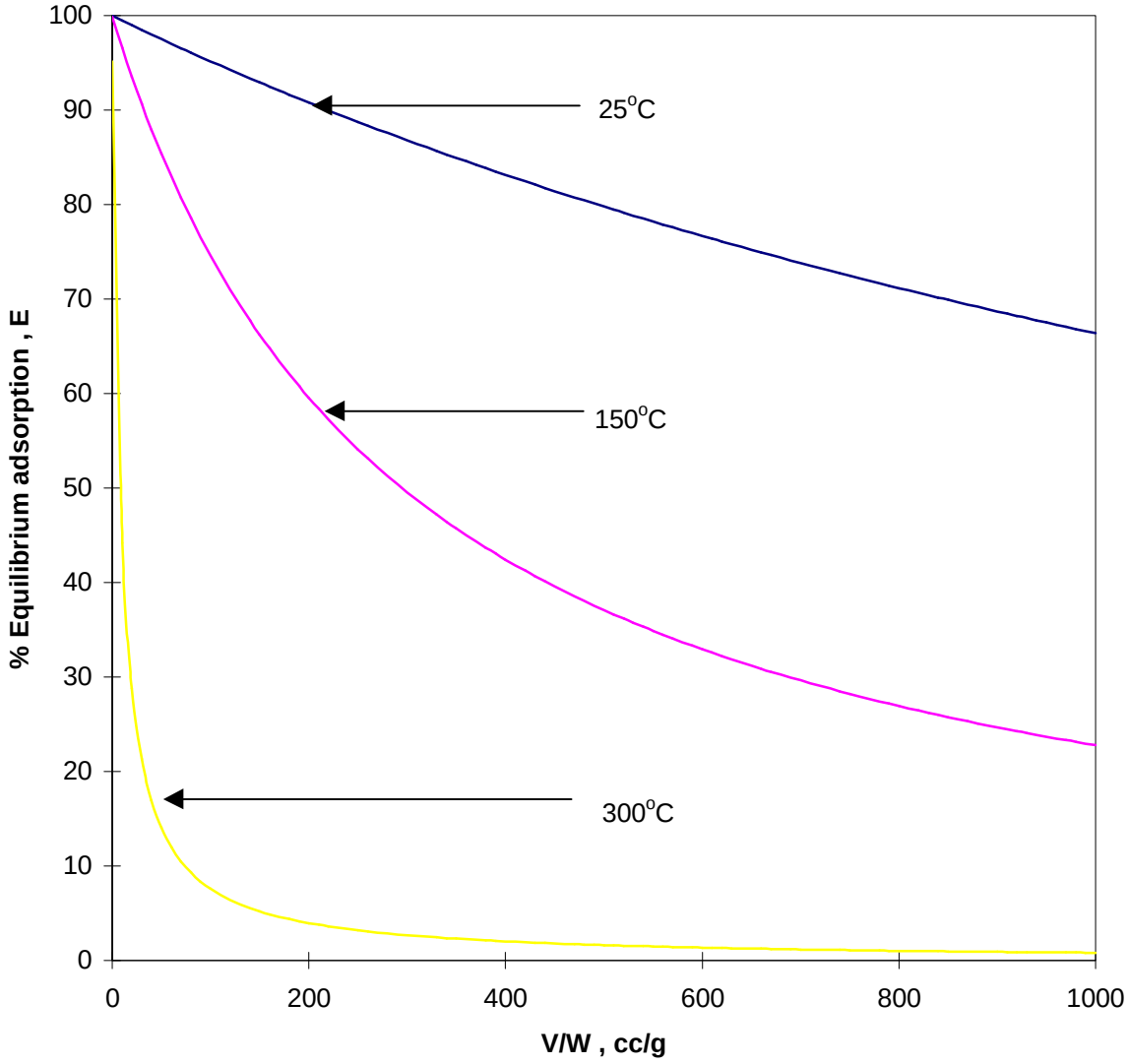

Figure 22. Equilibrium adsorption against V/W for the quinoline/mineral oil system at different temperatures.

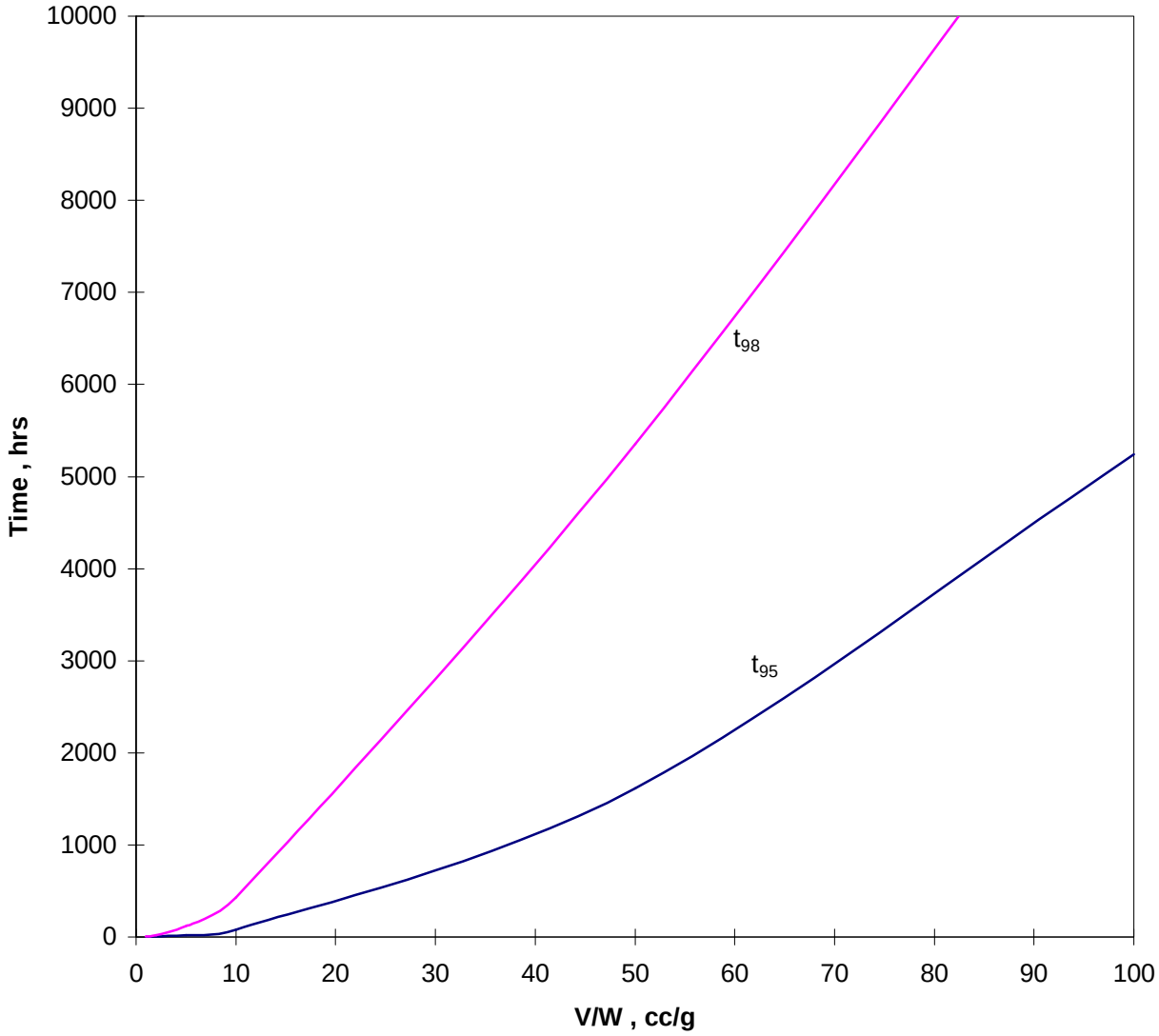

Figure 23. Equilibrium adsorption times for different values of V/W for the quinoline/mineral oil system at 25°C.

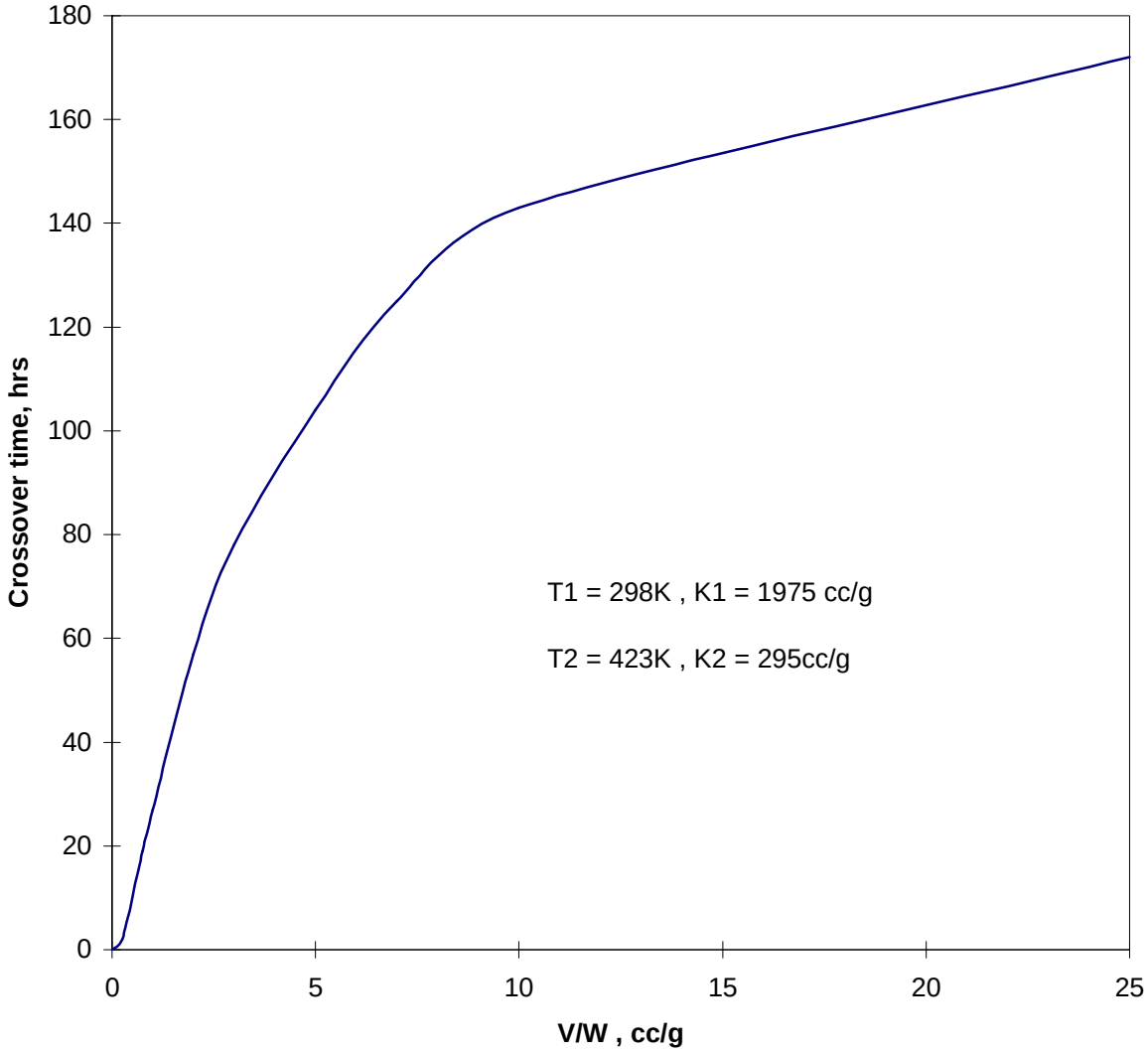

Figure 24. Model simulation of the crossover times for two different temperatures at different values of V/W for the quinoline/mineral oil system.

Planned Work

A no-cost extension has been obtained for this project which will allow Mr. Vadlamani to continue his work to complete requirements for his M.S. degree. During the next time period we plan to study the effect of solvent composition on the diffusion/adsorption uptake process using quinoline and solvents of mixed composition having a range of aromaticity. Following this work, it is planned to investigate the diffusion of asphaltenes in such mixed solvents at a range of temperatures.